



LAWRENCE
LIVERMORE
NATIONAL
LABORATORY

The National Ignition Facility System Alignment

S. Burkhart, E. Bliss, P. Di Nicola, D. Kalantar, R.
Lowe-Webb, T. McCarville, D. Nelson, T. Salmon, T.
Schindler, J. Villanueva, K. Wilhelmsen

August 27, 2010

Applied Optics

Disclaimer

This document was prepared as an account of work sponsored by an agency of the United States government. Neither the United States government nor Lawrence Livermore National Security, LLC, nor any of their employees makes any warranty, expressed or implied, or assumes any legal liability or responsibility for the accuracy, completeness, or usefulness of any information, apparatus, product, or process disclosed, or represents that its use would not infringe privately owned rights. Reference herein to any specific commercial product, process, or service by trade name, trademark, manufacturer, or otherwise does not necessarily constitute or imply its endorsement, recommendation, or favoring by the United States government or Lawrence Livermore National Security, LLC. The views and opinions of authors expressed herein do not necessarily state or reflect those of the United States government or Lawrence Livermore National Security, LLC, and shall not be used for advertising or product endorsement purposes.

The National Ignition Facility System Alignment

**S. C. Burkhart, E. Bliss, P. Di Nicola, D. Kalantar, R. Lowe-Webb, T. McCarville,
D. Nelson, T. Salmon, T. Schindler, J. Villanueva, K. WilhelmSEN**

Lawrence Livermore National Laboratory, P.O. Box 808, Livermore, CA 94551, USA

Abstract The National Ignition Facility is the world's largest optical instrument, comprising 192 – 40cm-square beamlines, each generating up to 9.6kJ of 351nm laser light in a 20ns beam precisely tailored in time and spectrum. The Facility houses a massive (10m diameter) target chamber within which the beams converge onto a ~1cm size target for the purpose of creating the conditions needed for deuterium/tritium nuclear fusion in a laboratory setting. A formidable challenge was building NIF to the precise requirements for beam propagation, commissioning the beamlines, and engineering systems to reliably and safely align 192 beams within the confines of a multi-hour shot cycle. Detailed within are the processes used, the major issues resolved, and the alignment results obtained during the decade of NIF construction, commissioning, and operations.

OCIS codes: [140.0140](#)

1. Introduction

NIF architecture and Facility

The National Ignition Facility (NIF) is the world's largest laser, designed to create fusion ignition and gain in a laboratory setting. The Facility (Fig. 1) was completed

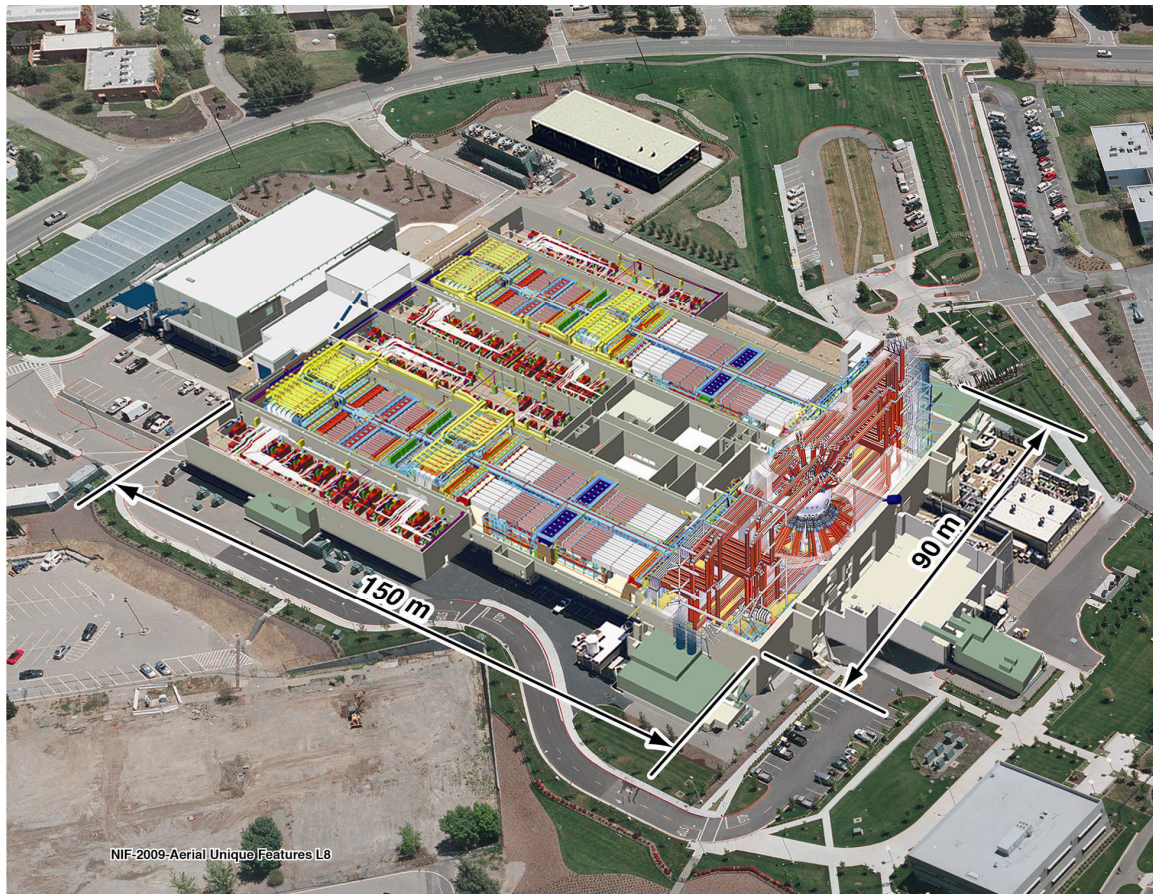


Figure 1. The NIF building is approximately 150 x 90 m, 7 stories tall. It comprises 11 sections; 2 laser bays, 4 power conditioning bays, 2 beam switchyards, a target bay, a diagnostic building, and a core controls and oscillator area. Supporting facility buildings include optical processing facilities for optical line replaceable unit assembly and acceptance testing, electrical and other specialized utilities, and office space. The roof is 'removed' in this view to facilitate the reader's understanding of the physical layout.

in February 2009. It consists of 192, 37cm-square laser beams arranged in four clusters, each comprising six bundles of two-by-eight beams, which are focused into a 10m diameter target chamber. It is a conventional flashlamp-pumped neodymium-doped phosphate-glass laser of unique four-pass design for its size. Each square 1053nm beam is multi-pass amplified through sixteen 810×460×41mm laser slabs (125 metric tons for all NIF), transported to the target chamber through beamtubes and 5 mirrors, frequency converted to 351nm, and focused on the target. The system is housed in a building 150m long by 90m wide, standing 4 m from the deepest point to the ceiling. An excellent description of the NIF architecture is provided in reference [1], and more description of the evolution and architecture is presented in reference [2]. On March 10, 2009 the system demonstrated performance of 1.1MJ of 351nm light to target chamber center.



Figure 2. Photograph of Laser Bay 2 from atop the main amplifiers. The large piping in the foreground is for amplifier and flashlamp cavity purge and cooling gas. The blue structures upon which the workers are standing are vacuum vessels for SF1, the first spatial filter lens. Mid-image is dominated by the amplifier cavity spatial filter tubes and central vessel. Beyond that is the rise of the periscope section within which resides the LM2, LM3, Polarizer, PEPC electronics racks, and PEPC, described later in the text. The Laser Bay to Switchyard wall can be seen at the far-end of the image.

Target experiments commenced in May, 2009 with a series of target design tuning shots followed by ignition and gain experiments planned for the latter half of 2010 and into 2011.

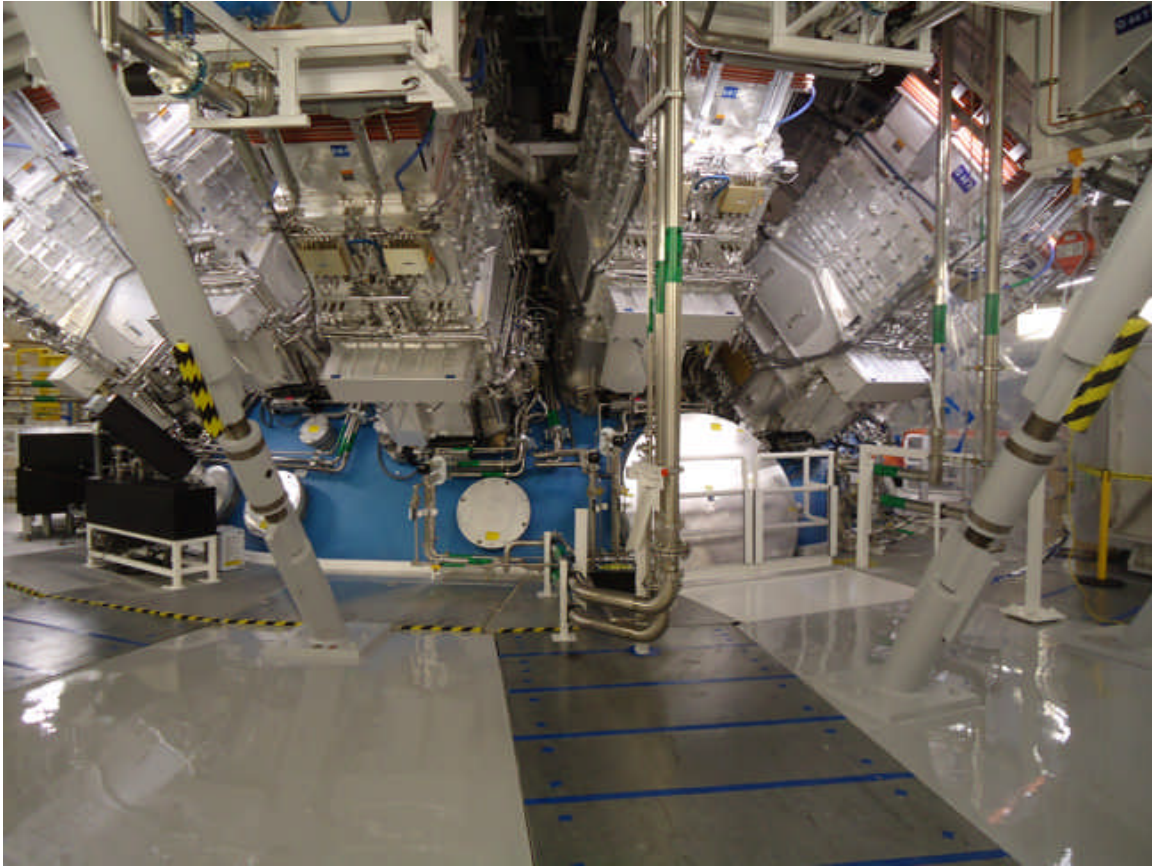


Figure 3. Upper hemisphere of the 10m diameter target chamber. Four beams at a time enter the chamber through the large, rectangular, Final Optic Systems (FOS) structures. They include optics for frequency conversion, phaseplate beam conditioning, vacuum barrier, focus, diagnostics, and debris protection. Note the large turnbuckles on the support members which were used for precise positioning of floor structures during construction.

Precise beam pointing requirements govern system alignment, as well as requirements for beam propagation pointing and centering for machine safety. In this paper we present the methods used to meet these beam pointing & centering requirements from initial construction to target shot operations.

NIF Alignment

As the world's largest optical instrument, NIF was a monumental challenge to design construct, commission, and transition to routine and safe operations. This paper is organized around four alignment phases

- 1) **Design: Vibration and drift design mitigation;** Beam pointing to NIF targets is required to be better than 50 μm RMS, driving a rigorous process of vibration and drift source isolation, coupling minimization, and system response control. Mirror stability was a primary consideration, as small angular deviations are multiplied by the target lens 7.7 m focal length to obtain the spatial deviation. Gas stability within the beampath was also important, for both pointing and wavefront stability. Lens stability was less of a concern, but it was included in the error budget. Stability design considerations are reviewed in detail in reference [3].
- 2) **Construction alignment;** NIF was constructed with the mirrors, lenses, alignment references and all other components positioned using precision survey techniques. The kinematic mounts for these optics were installed as much as 7 years prior to first beam alignment, and in certain cases were installed into assemblies at an off-site facility prior to installation. This required extensive precision survey networks supported by large crews of surveyors and a well-controlled mechanical model of the beampath hardware. The largest structures with precision alignment requirements were the 16 spatial filter end vessels (Fig. 4), each containing 48 lenses requiring $\pm 1\text{mm}$ 3σ (three times standard deviation) placement. These vessels and a large number of smaller ones were pre-aligned off-site in parallel with NIF construction, then placed in the NIF building using precision survey tolerances

throughout vessel placement. Error checking was employed throughout to ensure data integrity and verify compliance with alignment tolerances.

- 3) Commissioning alignment;** For initial beam alignment, or “Commissioning Alignment,” all or part of the beampath was prealigned, using one or more alignment beams, to tolerances permitting beam acquisition and automated beam alignment to function. Commissioning alignment fixtures, sources, and sensors were used to set mirror angles both offline (prior to installation) and online, and to precisely position injection and diagnostic lens cells.



Fig. 4. The vacuum vessels containing a cluster of SF4 Spatial Filter Lenses (see Fig. 5) were installed and precision aligned in 2001, with a $\pm 1\text{mm}$ requirement on lens center placement tolerance. They were commissioned for alignment and shots in 2008 with no further alignment.

- 4) Automatic alignment;** The final and operational phase of system alignment is automatic alignment, the process for autonomous beam alignment prior to system shots. A multiplexed suite of cameras, references and beam fiducials combined with

robust image processing provides feedback to motorized mirror mounts to center and point each beam. Commissioning effort for the Automatic Alignment System consumed 10's of man-years, but resulted in an autonomous alignment system capable of 192 beam alignment to Target Chamber within 60 minutes.

2. NIF Laser Architecture

No alignment review is possible without an architecture discussion, a summary of which is presented in this section.

A single NIF beamline is shown in Figure 5. Each beam starts at the Master Oscillator Room (MOR), within which are three oscillators – two for the Inner and one for the outer target chamber cones [4]. The oscillators [5] are of fiber-optic design with an architecture of amplification and beam conditioning to impart spectral and temporal features onto the beam as required by target physics constraints. A series of fiber splitters and amplifiers supply light to 48 individual quads of beams in the preamplifier. Each beam is temporally shaped prior to the preamplifier, with an injected energy of $\sim 300\text{pJ}$.

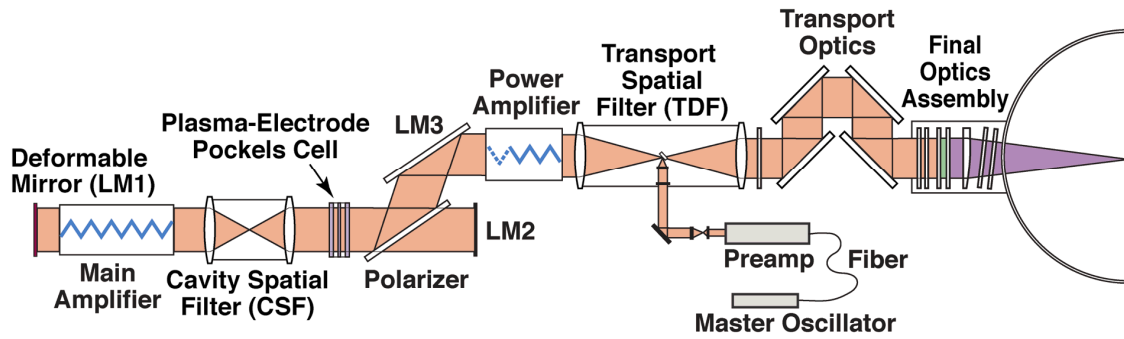


Fig. 5. Schematic layout for one of the 192 beamlines, from fiber oscillator to fusion target. The pulse is created, amplified and then injected into the Transport Spatial Filter. After four amplification passes in the cavity and two in the power amplifier, it is transported to the target chamber, frequency converted and conditioned, and focused onto the target.

The preamplifier [5] consists of first, a diode-pumped regenerative amplifier (Fig. 6) into which the precisely shaped and conditioned MOR pulse is switched by the Pockels Cell (PC1) and amplified through 57 round trips to $\sim 2\text{mJ}$. Switched out by PC1 and expanded $20\times$ to 18mm square, the beam is spatially shaped at the first optical relay plane (RP0) for the NIF laser system. Next, the four-pass, flashlamp-pumped Nd:glass rod amplifier cavity (Fig. 7) amplifies the beam to $\sim 2\text{J}$, and the beam power, energy, and near-field are acquired for analysis by the Input Sensor Package (ISP). Beyond the ISP, the beam is split 4-ways and image-relayed (Fig. 8) to the final relay plane (RP-10) prior to injection.

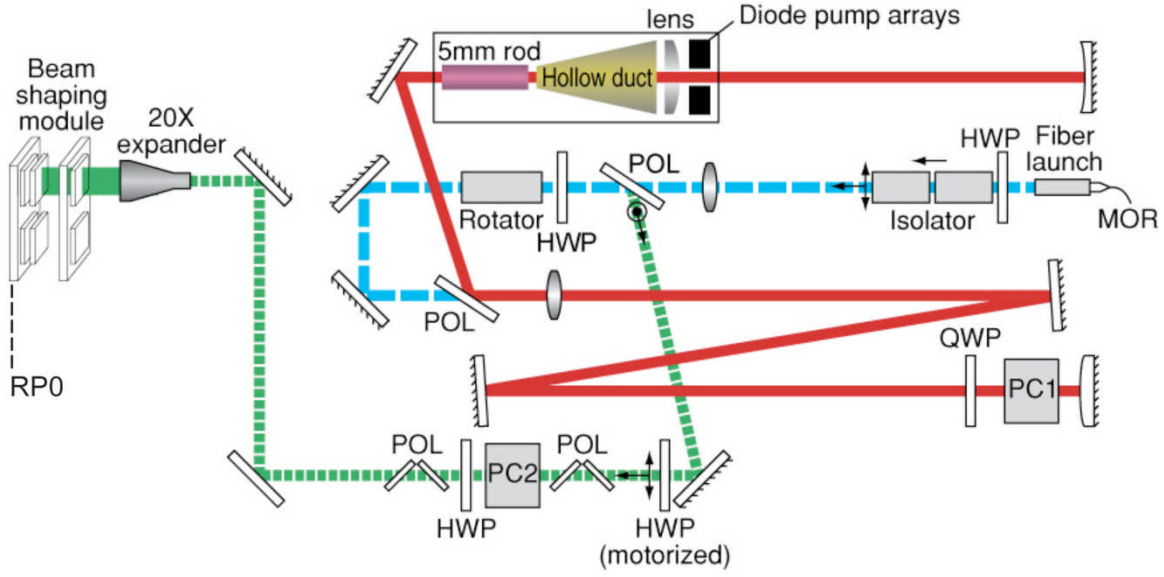


Fig. 6. Injection Laser System (ILS) regenerative amplifier. Light from the MOR fiber launch is collimated and injected through an isolator and polarizer into the main regenerative amplifier cavity. After the pulse passes through it, the Pockels cell PC1 is switched on, trapping the pulse in the cavity for 57 round-trips. During each round-trip, the pulse passes twice through a diode pumped rod amplifier. PC1 is switched off to transport the amplified beam to the output. A motorized half-wave plate in combination with a set of polarizers controls the energy transmitted to the next stage of amplification. A 20 \times beam expander in combination with a beam-shaping module spatially shapes the beam to the desired profile.

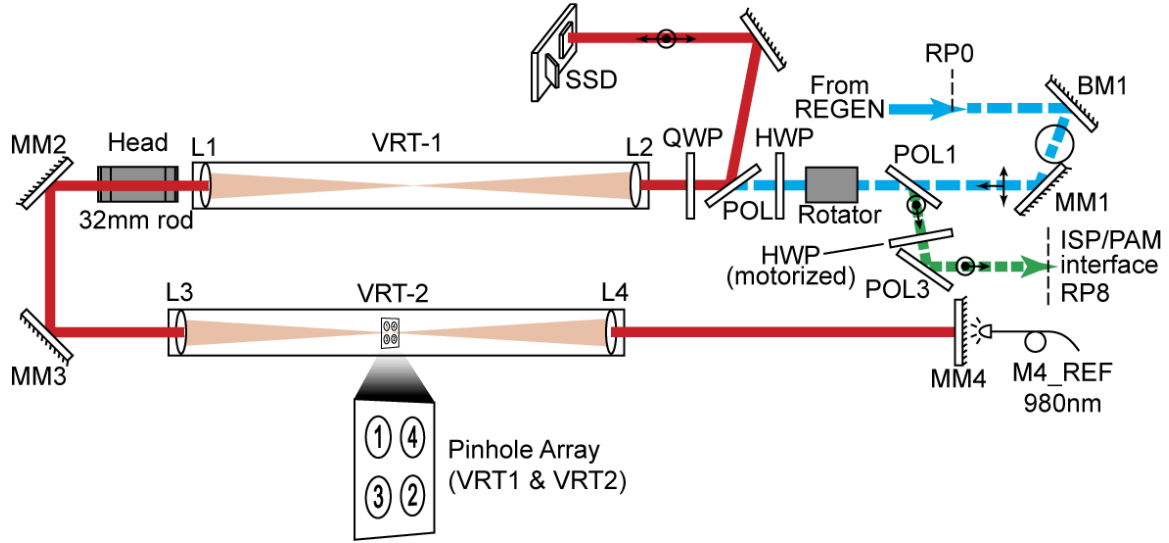


Fig. 7. There are 48 multi-pass pre-amplifiers for NIF, one for each quad of beams. Light from the preceding regenerative amplifier is amplified to approximately 2J through 4-passes within the 32mm-diameter flashlamp-pumped rod amplifier.

Beam injection into the main laser (Fig 8) is accomplished by matching to the f/no. of the 30.15m focal length Transport Spatial Filter (TSF) lenses and injecting off a mirror positioned near the TSF pass-1 focus. The injection focus is laterally displaced 17.5mm from the TSF optical centerline, which defines the angular separation of multiple laser passes. Therefore, the output beam focus is aligned 35mm laterally from the injection beam in the TSF. Expanded to 372mm, the beam is collimated then amplified through the five pumped slabs of the Power Amplifier (Fig. 5). After the beam enters the four-pass cavity by reflection off of LM3 and the Polarizer, it passes through the 11.8m focal length cavity spatial filter (CSF) pass-1, and through eleven pumped slabs to LM1, which is also a deformable mirror [6] for wavefront correction. LM1 re-points the beam back through pass-2 of the CSF.

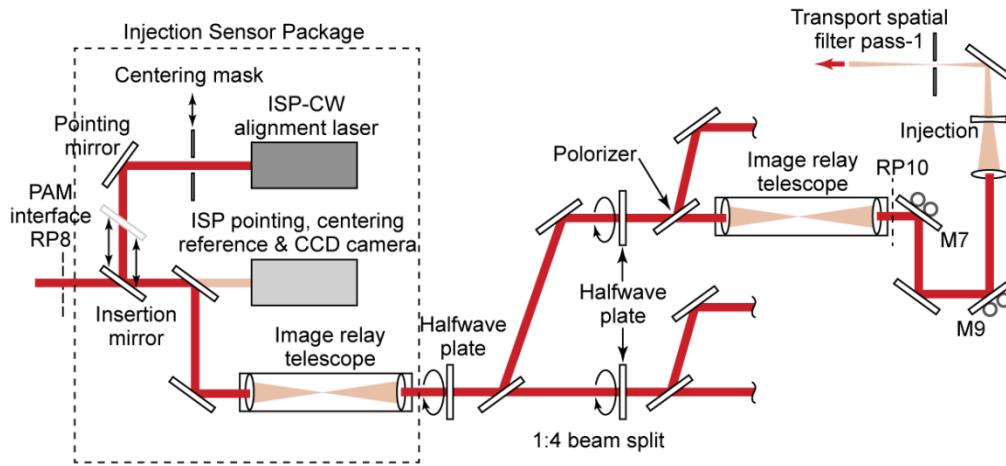


Fig. 8. The output from each preamplifier module (PAM) is aligned to the Injection Sensor Package (ISP) centering and pointing references, as is the ISP-cw alignment laser. Then the 48 beams undergo a $4\times$ split prior to alignment into the each of the 192 Main Laser Transport Spatial Filters.

During the 280ns beam round-trip to LM1, the Plasma Electrode Pockels Cell (PEPC) [7] is activated, rotating beam polarization 90° to pass through the polarizer to LM2. LM2 points the beam through CSF pass-3, followed by a second reflection off LM1 through CSF pass-4. Between passes 3 and 4, the PEPC is de-energized, so that pass-4 reflects off the polarizer and LM3, returns for a final pass of the five pumped slabs of the Power Amplifier, and out through the TSF pass-4 pinhole, thus completing the main laser amplification process. NIF uses $200\mu\text{R}$ radius pinholes for all but TSF pass 1, which is $100\mu\text{R}$.

Once recollimated by the TSF output lens, the beam passes into the NIF Switchyard and target bay (Fig. 9), where the rectangular array of 192 Main Laser beams is remapped to

match the spherical geometry of the target chamber. Each beam reflects from 2 mirrors in the Switchyard, and two (or three) in the Target Bay. The final mirror is positioned to send the beam through Final Optics System (FOS), to Target Chamber Center (TCC).

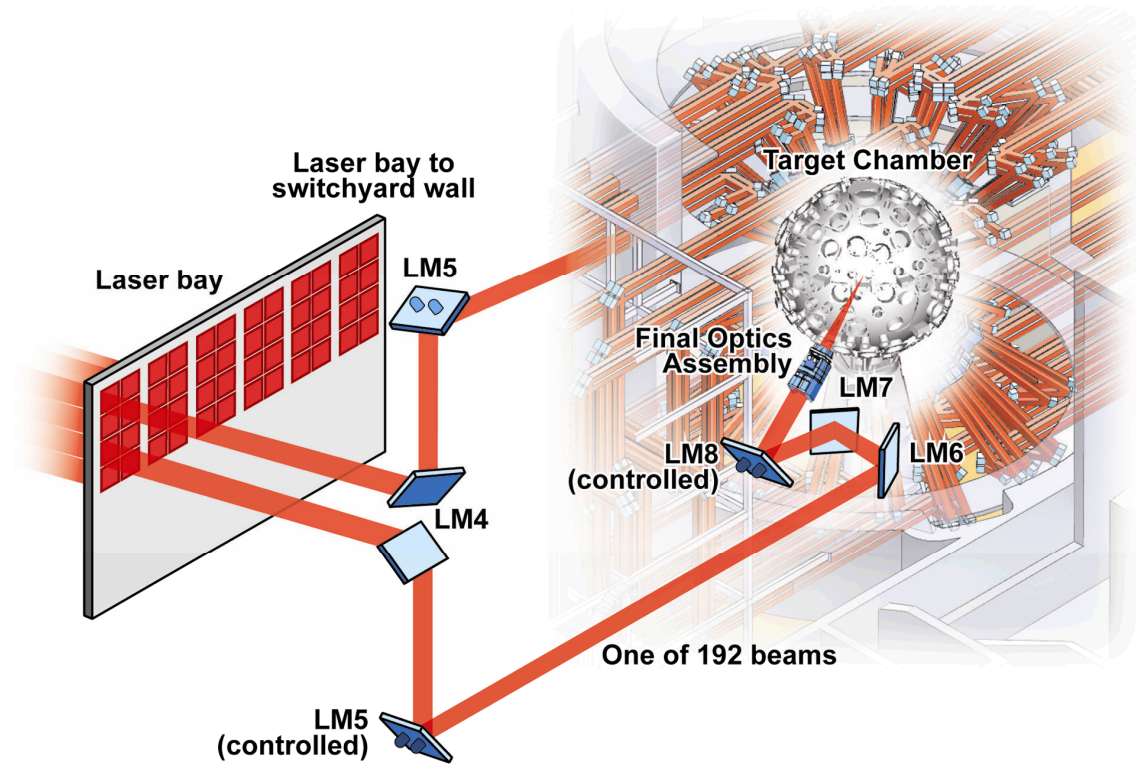


Fig. 9. Beams are transported to the final optics by mirrors LM4 – LM8. Mirrors LM5 and LM8 comprise the remotely-actuated gimbal pair for alignment to TCC.

The FOS (Fig. 10) consists of 6-8 full-aperture optics, depending on the particular required beamline configuration. These optics provide beam conditioning [8] (phase-plate), the vacuum barrier, frequency conversion from 1053 nm to 351 nm [9], beam focusing and color separation using a wedged lens, diagnostic sampling using a low-efficiency grating, and target debris protection. Haynam et al. [10] presents performance results for a single beamline on which NIF laser requirements for a single beam were

achieved in 2006. NIF performance to 1.1 MJ for all 192 beams simultaneously was achieved on March 10, 2009.

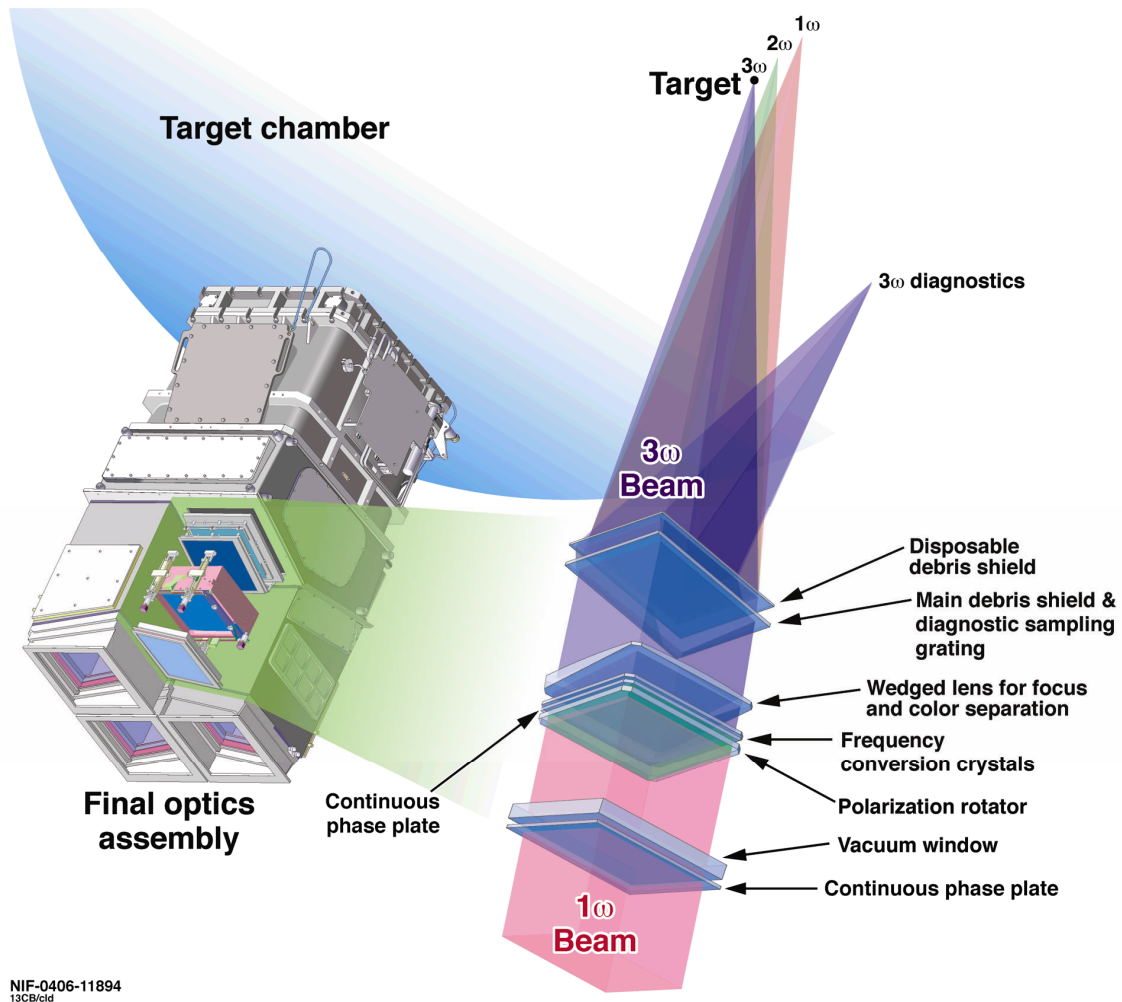


Fig. 10. A series of fused-silica and KDP optics comprise NIF final optics as detailed here. The continuous phase plate is in one location or the other, never both, and the polarization rotator is present for only half the beams.

3. NIF Alignment Process

Vibration and drift design mitigation

NIF pointing and clear aperture requirements were established early in the NIF design cycle, in order to provide optical and mechanical engineering design guidance. Beam pointing is much more susceptible than beam clearance (clear aperture) to vibration, and thus is the primary constraint on vibration and drift. The requirements are:

- Point the focused beam to within 10% of the Cavity Spatial Filter (CSF) pass 1 and pass 2 pinhole diameters [11], or $\pm 40\mu\text{R}$ for the $200\mu\text{R}$ radius pinholes.
- Point the focused beam to within 5% of the CSF pass 3 and pass 4, and TSF pass 1 and pass 2 pinhole diameters [11], or $\pm 20\mu\text{R}$ for all except the $100\mu\text{R}$ TSF pass 1, which is $\pm 10\mu\text{R}$.
- Point the focused beam to the target to better than $50\mu\text{m}$ RMS when measured perpendicular to the beam propagation direction [12]. For the NIF 7.7-m final focus lens, this becomes $\pm 6.5\mu\text{R}$, the dominant pointing requirement.

The pointing requirements within the laser exist for safe laser operation, as beam clipping at a pinhole or other location is potentially damaging to downstream optics. However it is pointing to the Target Chamber Center that drives alignment performance. Budgeting within the areas contributing to the top-level $\pm 50\mu\text{m}$ RMS beam positioning was managed using Table 1, accounting for all misalignment contributions. Terms corresponding to alignment, vibration, and drift (Fig. 11) were summed either in quadrature or directly as described by Sommer and Bliss [13].

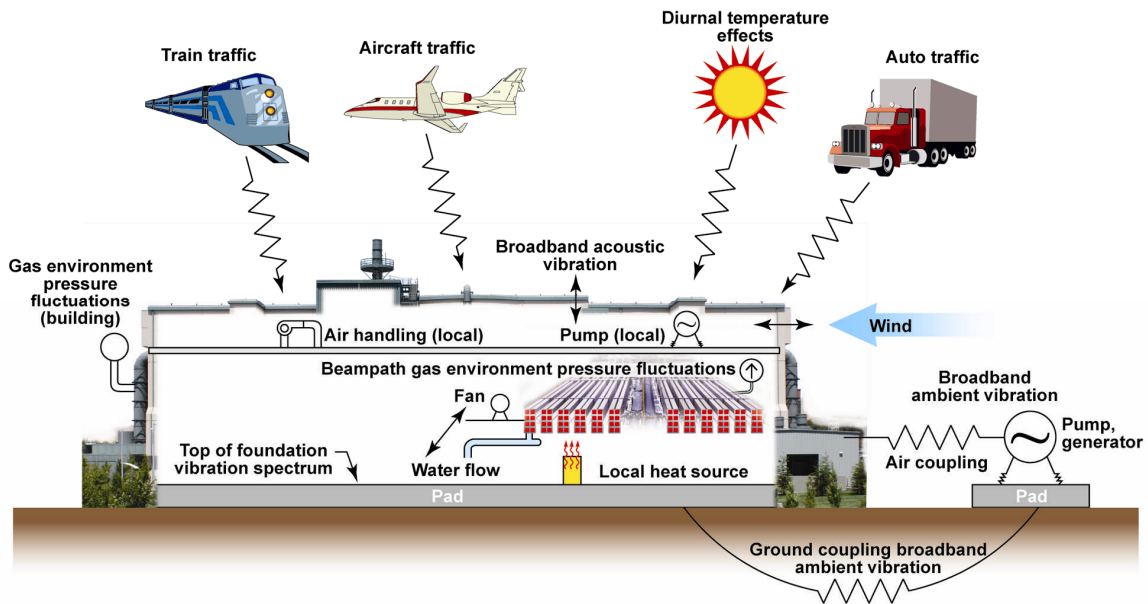


Fig. 11. Alignment perturbing effects from all possible man-made and natural effects were assessed and reduced by mitigation at the source (if possible), by limiting the coupling into the facility and to the structure, and by designing the alignment-sensitive structures to have the minimum response.

Vibration and drift effects on alignment were considered based upon the following categories:

Vibration pointing errors (>2 Hz)

Broad Band Ambient Vibration – Vibration contributions from sources external to the NIF building, including rotating equipment, automobiles, trucks and trains. This source is summarized by a “top of foundation” vibration spectra [14], [15] and is all assumed to be coupled through the soil [16].

Local Vibration – Sources internal to the NIF building, including heating and ventilation (HVAC) systems, pumps, clean room and cooling fans, and fluid and air flow, which can couple through support structures to sensitive optics.

Broadband acoustic vibration – Air-coupled vibration, from external or local sources.

We found such sources on previous laser systems [17] where 14Hz acoustics from the building heating and ventilating system coupled all too well into a 14Hz enclosure/mirror response. Aircraft noise falls into this category.

Gas environment pressure fluctuations – Building or beampath enclosure pressure changes affect support structures and beam pointing.

Target Bay & Switchyard acoustic vibration – Separately tabulated broadband acoustic vibration.

Target Bay & Switchyard wind vibration – Separately tabulated wind effects.

Target Bay & Switchyard pressure fluctuation – Separately tabulated building and enclosure pressure fluctuations.

Drift pointing errors (<2 Hz)

Diurnal temperature caused drift – Radiation from ceiling and wall heating affects local beamline support structures.

Internal HVAC temperature caused drift – Beamline support structures affected by HVAC temperature fluctuations.

Local transmitted temperature drift – Local heating or cooling due to electrical, gas, or cooling water effects, as it affects system pointing.

Beam alignment tolerances affecting pointing to TCC are also entered in Table 1. The source of these uncertainties is the NIF architecture and the alignment methodology, whereby two separate cw sources (not the pulsed beam) are used for beamline alignment. There are two separate co-alignment locations with four error terms that add to pointing

error on target. (described later). In addition, the uncertainty or error in target alignment to TCC is included in Table 1.

Extensive design measures were taken to ensure NIF met its criteria for “top of foundation” vibration specifications. NIF utility systems were remotely located from the NIF building to the greatest extent possible. Rotating equipment, whether remote or within the NIF building, used compliant mounting techniques. HVAC acoustic modes were modeled and mitigated, and all structures had structural modal analysis to keep structure response to the “top of foundation” excitation within the limits originally specified in Table 1. Validation through measurement, calculation, or a combination of the two was performed for about half the Table 1 assumptions [14], [15] showing overall compliance to the original assumptions published by Sommer and Bliss.

Table 1: Pointing Stability Budget Allocations																		
fTar = Focal Length (Target) =		7.7 m																
fCSF = Focal Length (CSF) =		11.756 m																
fTSF = Focal Length (TSF) =		30.15 m																
Source error term	Alignment Error, ref. To TCC (um)	Broad Band Ambient Vibration (BBAmV)	Local Vibration (LV)	Broad Band Acoustic Vibration (BBAcV)	Gas Environ. Pressure Fluc. (GEPF)	TB/SY Acoustic Vibration (TBSYAV)	TB/SY Wind Vibration (TBSYVW)	TB/SY Pressure Fluc. (TBSYPF)	Total Drift due to Vibration & Pres. Fluc. (Drift V&PF)	Diurnal Temp. Change (DTC)	Internal HVAC Trans. Temp. Change (IHTTC)	Local Trans. Temp. Change (LTTC)	Total Thermal Drift (Drift /Thermal)	Total Error	Multiplier to convert source error term to error at target	Multiplier value	Error at Target (microns)	Percentage
MPA Output Pointing handoff	6.40													6.40	1	1.000	6.40	1.48
TSF Pass 4 pointing error	11.05													11.05	1	1.000	11.05	4.40
375nm pointing error at the T	7.01													7.01	1	1.000	7.01	1.77
Target positioning/alignment	6.80													6.80	1	1.000	6.80	
375nm to Pulsed beam compo	9.42													9.42	1	1.000	9.42	3.20
OSP (uR)									0.60					0.60	fTar	7.700	4.62	
PAM (uR)									1.03					1.03	fTar	7.700	7.93	
ISP (uR)									0.21					0.21	fTar	7.700	1.62	
PABTS (uR)									0.56					0.56	fTar	7.700	4.31	
Inj_Optics (uR)									0.19					0.19	fTar	7.700	1.46	
LM1 (uR)		0.20	0.05	0.05	0.11				0.24		0.22	0.02	0.24	0.34	2*2*fTar	30.8	10.41	3.90
LM2 (uR)		0.12	0.00	0.10	0.05				0.16		0.19	0.02	0.21	0.27	2*fTar	15.4	4.10	0.61
LM3 (uR)		0.19	0.00	0.10	0.05				0.22		0.19	0.02	0.21	0.30	2*2*fTar	30.8	9.28	3.11
Polz (uR)		0.18	0.00	0.10	0.05				0.21		0.19	0.02	0.21	0.30	2*2*fTar	30.8	9.11	3.00
OPG (microns)		2.80	0.00	1.00	0.50				3.01		1.70	0.20	1.90	3.56	fTar/fTSF	0.25539	0.91	0.03
SF1(microns)		0.65	0.00	1.00	0.50				1.29		1.70	0.20	1.90	2.30	4*fTar/fCSF	2.619939	6.02	1.31
SF2(microns)		0.65	0.00	1.00	0.50				1.29		1.70	0.20	1.90	2.30	4*fTar/fCSF	2.619939	6.02	1.31
SF3(microns)		0.74	0.00	1.00	0.50				1.34		1.70	0.20	1.90	2.33	2*fTar/fTSF	0.510779	1.19	0.05
SF4(microns)		0.74	0.00	1.00	0.50				1.34		1.70	0.20	1.90	2.33	fTar/fTSF	0.25539	0.59	0.01
LM4 (microradians)		0.22	0.00	0.10	0.05	0.15	0.03	0.01	0.29	0.02	0.13	0.02	0.17	0.33	2*fTar	15.400	5.15	0.96
LM5(microradians)		0.26	0.00	0.08	0.05	0.00	0.03	0.01	0.27	0.08	0.13	0.02	0.23	0.36	2*fTar	15.400	5.52	1.10
LM6(microradians)		0.21	0.00	0.14	0.05	0.15	0.15	0.15	0.36	0.15	0.24	0.02	0.41	0.55	2*fTar	15.400	8.43	2.56
LM7(microradians)		0.21	0.00	0.14	0.05	0.15	0.15	0.15	0.36	0.15	0.24	0.0						

19

The NIF facility design is tied to a group of Optical Configuration Drawings (OCD's) (excerpt in Fig. 12), which define the coordinates for each optic in the 192 laser beams. These drawings include only the optics, the beam centerline, and the position of the optics relative to that beamline. All other mechanical designs and drawings including optical lens mounts, supports, beam enclosures, pedestals, indeed the building itself are all designed around the OCD. Thus precise initial placement of all support structures was required to meet OCD requirements.

The NIF facility design is tied to a group of Optical Configuration Drawings (OCD's) (excerpt in Fig. 12), which define the coordinates for each optic in the 192 laser beams. These drawings include only the optics, the beam centerline, and the position of the optics relative to that beamline. All other mechanical designs and drawings including optical lens mounts, supports, beam enclosures, pedestals, indeed the building itself are all designed around the OCD. Thus precise initial placement of all support structures was required to meet OCD requirements.

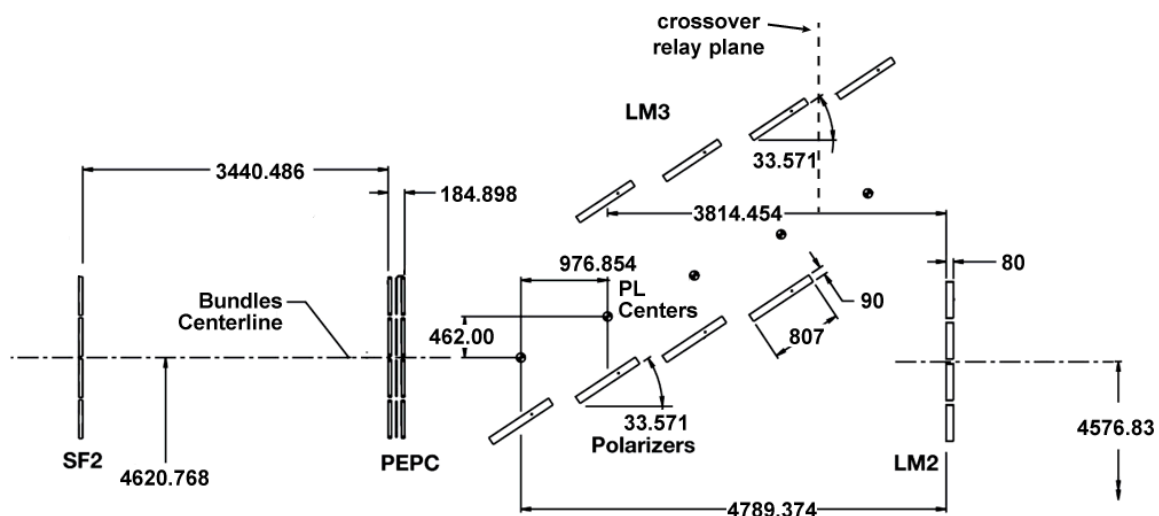


Fig. 12. The NIF design is tied to optical configuration drawings (OCD's). An excerpt from the main laser OCD is shown here. The position of each beam in space and the beam centers on mirrors, lenses, and other optics are controlled by design, and all other structures including the building were designed around the optical configuration.

From the outset it was clear that conventional optical alignment strategies were inadequate for positioning the large (400mm+) optical components in the main beamline.

By traditional alignment we mean establishing beam centerline with a pilot beam, and installing components to that beam. On NIF, the lenses, pinholes, mirrors and alignment references were not designed for personnel access. Thus alignment similar to NIF's predecessors such as NOVA was not possible. We chose instead to utilize precision survey techniques, to position or place the beampath structures.

Precision survey, differentiated here from conventional survey, utilizes automated laser trackers and precision retroreflectors, and involves multiple measurements to each survey monument. The multiple measurements are 'best-fit' using weighted least-square methods to obtain both a best estimate of position and a calculated uncertainty.

NIF coordinate generation, to specify component installation locations, was a very disciplined process of parametrically linking system mechanical designs and drawings to assure consistent system interface coordinates. Thus, our process was to a) develop a precision survey network, b) implement disciplined coordinate control of NIF beampath-related mechanical designs and c) position critical mechanical components precisely within this system.

Survey network development. The NIF precision survey network, a building-wide precision coordinate system, was developed in phases with three distinct networks; Basic, Intermediate, and Precision, not including initial construction site land survey. NIF site survey began in 1996, with construction monuments established from conventional land survey monuments. These were valued to .005 ft (land surveyor parlance) and used for

site preparation including grading, excavation, and locating of the Laser and Target Area Building (LTAB) walls and ancillary facilities. Almost immediately, however, the critical difference between the NIF site and normal construction sites was made apparent. During initial grading, one key monument was inadvertently pushed 1 inch upward by nearby site construction traffic resulting in sections of the NIF site grade being 1” too high. At other sites, the construction could perhaps adapt to such a ‘minor’ offset, but for NIF the contractor was required to lower the LTAB grade by the 1” discrepancy. Following grading, the construction monuments were used to locate the LTAB wall foundation footings, and the LTAB wall structural steel was subsequently erected.

Within the wall structural steel boundaries, approximately 130 survey network monuments for the NIF survey network were installed in the footings. These survey network monuments (SNM’s) were ‘valued’ (coordinates established) by incorporating a best-fit of the building structural steel “as-built” coordinates into the design. Values were then assigned to each SNM accordingly. This completed, the Survey Network was effectively severed from that point forward from external references (outside the LTAB) with a temporary exception for the switchyard and target areas. Network monuments outside the building were no longer needed for laser systems construction. This was called the ‘Basic’ network, and was used to locate the laser bay and core area floors, beampath support ‘pedestal’ structures, and the embedded steel brackets onto which beampath systems were later attached. The exception noted above was that switchyard and target area embeds and target area wall beam penetrations were positioned using external survey monuments – tied back to the Basic network.

With floors, pedestals, and embeds completed, an ‘Intermediate’ network was established. This had to be done before the wall interior panels were installed, as once that was done no further reference could be made to the Basic network SNM’s in the wall footings. Over 1000 SNM’s were installed in the laser bay floors and pedestals, in the switchyards, and target area, and then valued to a best-fit to the Basic network, a task requiring 32 surveyors and assistants for 10 days using laser trackers, total stations, and levels. For the Intermediate network the 3σ goal (3 times standard deviation uncertainty) was 3mm, as LTAB temperature control was not yet available. This requirement was surpassed, as we achieved 1mm, 3σ .

The Intermediate network was short-lived, as work began immediately on the Precision Network needed for beampath enclosure placement. Additional SNM’s were installed but not valued immediately, until temperature stability was achieved. Approximately 36 hours after the heating/ventilating/air-conditioning (HVAC) control began, thermistors embedded in the LTAB floor showed temperature stability was achieved deep within the floor, and the Precision Network survey began. Starting with Laser Bay 2, the dense network of SNM’s was surveyed and then valued from a best-fit to the Intermediate Network SNM’s. A 3σ goal of 300 μ m was more than achieved with a 185 μ m, 3σ Precision Survey Network. Improved techniques were used in Laser Bay 1, and 155 μ m, 3σ was achieved. It required 12 surveyors and three weeks for the Laser Bay 2 Precision Survey Network. Overall 6000 SNM’s were installed and valued throughout the LTAB at

a range of elevations. The switchyard goal was 1mm, 3σ , and we achieved 500 μ m, 3σ . The Target area goal was 300 μ m, 3σ , and we achieved 200 μ m, 3σ .

A significant requirement was the interface between the Laser Bay and Switchyard sections of the Precision network. This was driven by the first mirrors in the Switchyard (LM4s), which had a 4mm position tolerance and had to be aligned to the Laser Bay output, with no active adjustment possible because of the NIF laser architecture. Connection between the networks was made by surveying through open doorways, roll-up doors, and an open elevator. Shortly after the intermediate network was completed, we detected a subsidence of the Switchyard and Target Area portion of the LTAB relative to the Laser Bay survey network. Based upon the observed subsidence rate, we made a global adjustment to the Switchyard and Target Area coordinate system. Originally, the design center of the target chamber (TCC) was positioned 23' 0" above the Laser Bay floor (projected into the Target Bay), or 23' vertically from (0,0,0) in the NIF Global Coordinate System. This put TCC at (0, 7010.4, 186000) mm from the NIF Global coordinate origin. After the global adjustment, we modified it 10.4mm downward to put TCC at (0, 7000, 186000) mm. That change assumed the subsidence rate would continue at the same rate, with our best estimate as to where it would stabilize. The extent of the subsidence was realized as the first beams were sent through the laser-bay/switchyard wall and their position at LM4 was measured. In Cluster 3, we found the beams an average 6.2mm low at LM4, and for Cluster 4 they averaged 3.9mm low showing that we over-corrected. None of the beams exceeded the 8.1mm maximum allowable offset from a clear aperture analysis, although the vertical bias was less than ideal. Because of this

discovery, we resurveyed the positions of the transport spatial filter lens vessels in Switchyard 1 (SY1) to update the SY1 LM4 kinematic mount locations prior to their installation. We measured Laser Bay 1 SF3s to be 0.5 to 1.5mm low, and SF4s to be between 1.5 and 2.5mm low across the Cluster-wide spatial filter lens vessels. Applying beam perturbation based upon the sensitivities and accounting for the measured correlation between the laser bay and switchyard networks, we calculated an average 3.45mm offset for cluster 1 (CL1) and 3.75mm for CL2 LM4s, an offset consistent with our observations in CL4. We modified the design locations for the CL1 and CL2 LM4 kinematic mounts by linear interpolation across each cluster based upon these calculations, to optimally place the LM4s.

The subsidence in the region of SF3 to SF4 can be traced to an early NIF construction decision. While most of the Laser Bay concrete slab was built upon graded and compacted but otherwise virgin earth, the region near the Switchyard was excavated and later backfilled to facilitate construction of the wall from the 0' elevation Laser Bay floor to the -21'9" Switchyard floor. Unfortunately the best construction compaction practices do not compare to millennia of natural compaction, resulting in the ~2mm subsidence at SF4.

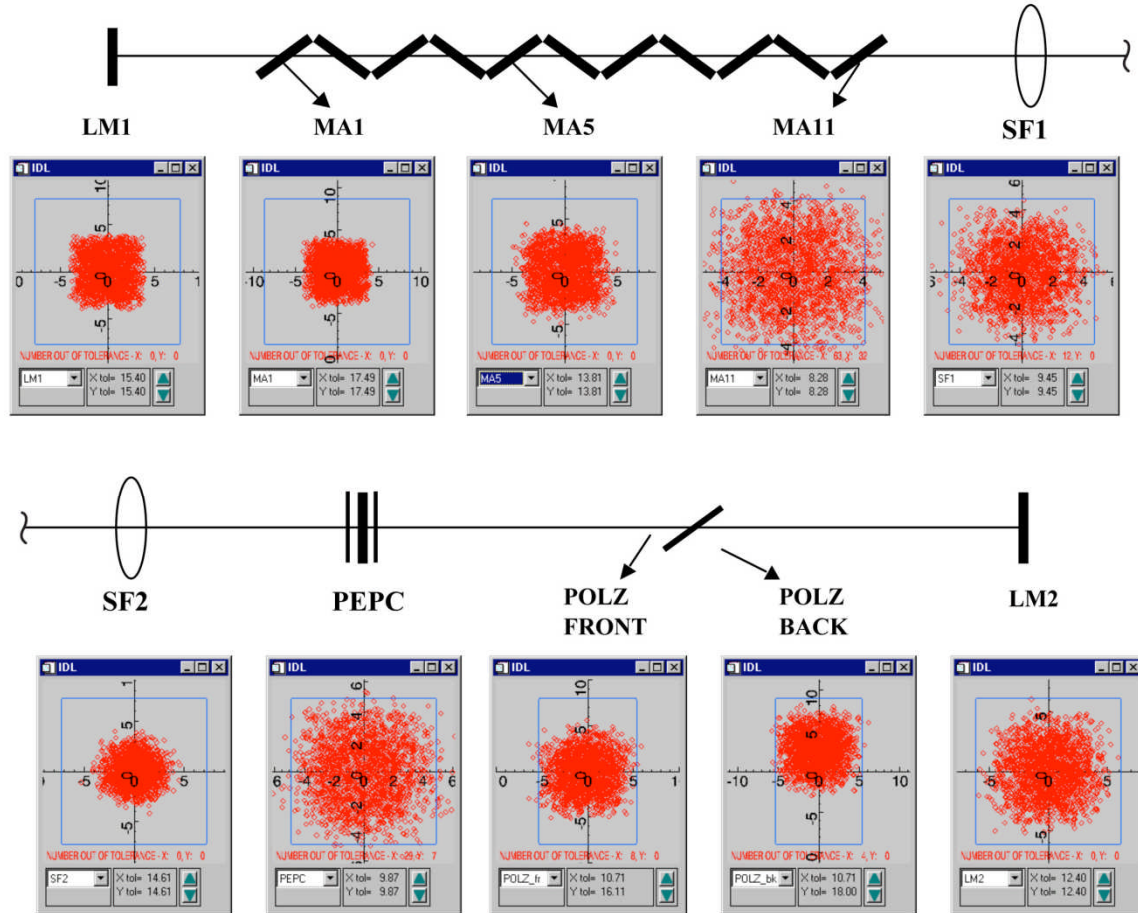
One other issue of note was either subsidence or compression of the Target Area building concrete. This concrete was designed 6 feet thick for neutron shielding, adding a tremendous weight to the base pedestal. Compression, settling, and adjustment of the Laser/Target vertical offset resulted in 30 lower Target Wall beam/quad penetrations

having 1cm to 5cm interference with the designed ‘through-the-wall’ beamtubes. In late 2000, we removed the interfering concrete to recover the required clearances.

Beampath vessel and component placement. The basic NIF Optical design [18] was used to set the alignment-specific requirements on optical component placement and tolerancing. Placement of alignment references, lenses and fixed mirrors as well as residual or design wedge tolerance on other transmissive optics combine to deviate the beam position throughout the laser. This was first analyzed for the main laser in 1996 [19] to set and validate the tolerances, and extended in 2000 [20] to include terms to target chamber center (TCC). Optic dimensions and design tolerances were finalized based upon the 1996 analysis, but in 2000 we revalidated the design, determining the expected deviation of the beam center at each of the large optics on NIF. The available beam size through the laser chain is reduced by expected beam alignment deviation at the limiting component. Stated otherwise – the component (lens, mirror etc) aperture less the beam deviation is the available beam size.

Using alignment, positioning, and tolerancing from [20], a Monte-Carlo analysis using boxcar tolerancing (hard \pm limits) for each term was performed [21]. Convolution would work just as well, but we chose a Monte-Carlo approach. (RMS works only for convolving normal tolerance distributions). Example results are shown in Figure 13, showing that the design constraints were adequate for most optics, with outliers on some components. Outliers have been mitigated by a commissioning step in which an alignment/centering offset, which centers the beam in each beamline, was implemented

in the alignment database. In addition, the actual NIF beamsize is smaller than the original worst-case assumptions, yielding additional margin.



BEAMLINE 111. Top beam (polarizer closest to LM2), shortest SF4-LM4, has an LM6, and an LM8 relatively close to FOA.

Fig. 13. Beam center on the main laser cavity optics was modeled through Monte-Carlo application of design tolerances for fabrication and positioning. This shows the result for beam center for 2000 Monte-Carlo samples, the tolerance at each optic is shown as the bounding box.

With completion of the precision survey network as described in the previous section, the local SNM's were used to position the vessels and enclosures in the building according to design. The enclosures and vessels, their quantity and positioning requirements were:

- Laser Mirror 1 enclosure (4) $\pm 0.5\text{mm}$
- Main Amplifier ‘Frame Assembly Units’ (24) $\pm 0.3\text{mm}$
- Cavity Spatial Filter Lens vacuum Vessels (8) $\pm 0.2\text{mm}$
- Cavity Spatial Filter center vessels (4) $\pm 0.2\text{mm}$
- Periscope vessels (4) $\pm 3.0\text{mm}$ (internal kinematic mounts individually surveyed to $\pm 0.1\text{mm}$)
- Power Amplifier ‘Frame Assembly Units’ (24) $\pm 0.3\text{mm}$
- Transport Spatial Filter Lens vessels (8) $\pm 0.2\text{mm}$
- Transport Spatial Filter center vessels (4) $\pm 0.2\text{mm}$
- Switchyard and Target area transport mirror LRU’s (320) (kinematic mounts individually surveyed to $\pm 0.14\text{mm}$)

These positioning requirements were derived from the top-level positioning requirements for lenses and alignment references ($\pm 1.0\text{mm}$), laser mirrors and laser slabs ($\pm 3.0\text{mm}$), and transport mirrors ($\pm 4.0\text{mm}$), which were used in the above validation. The tight requirements for the enclosures and vessels were dictated by the survey network uncertainty and the stack-up of mechanical uncertainties measured from the SNM to optic center (both RSS and direct sum). This ensured that the top-level requirements were met.

In order to place these vessels to the required precision, they needed to be measured offline prior to installation, and have precision survey features affixed in a location observable from a strategic and stable location. Typically we surveyed from the floor in the Laser Bay or attached to primary vertical structural steel in the Switchyards. The

spatial filter vessel and enclosure coordinates were established by precision survey in a remote building, in order to define coordinates for precision survey features on the vessels relative to lens kinematic mounts. The most complicated were the spatial filter lens vacuum vessels (Fig. 4). Each vessel precisely supports 48 spatial filter lenses to $\pm 1\text{mm}$, while maintaining high vacuum ($<10^{-4}$ Torr). As the kinematic mounts are not accessible at the time of vessel installation, a pre-installation survey process was followed to create external precision survey features (PSFs) used for vessel placement. The process was:

1. The vessel was positioned on temporary supports in a temperature controlled environment, and shimmed to remove vessel twist, as measured by precision survey instrumentation.
2. The PSFs were attached to the vessel at locations permanently observable to Precision Survey for vessel installation.
3. The vessel's beampath openings for the Spatial Filter Lenses were measured by Precision Survey, with the resulting data 'best-fit' into the design model for an installed vessel. The PSF's were temporarily valued accordingly.
4. Kinematic mounts, upon which the Spatial Filter Lens "Line Replaceable Units" (LRUs) sit for all 48 lenses (12, 4×1 Lens LRUs), were mounted and precision positioned in the frame of reference provided by the PSF temporary network.
5. Once all kinematic mounts were installed, a verification survey of the Kinematic Mounts was performed and 'best-fit' into the Kinematic Mount design locations.

The local network was adjusted to this new ‘best fit’ and the external PSFs re-valued to the revised network.

Thus, with the vessel PSFs valued to the kinematic mount best fit, the vessel was installed in the LTAB with no mechanical stack-up uncertainty, only the installation survey and the offline survey uncertainty between the PSF and kinematic mount positions.

A similar process was performed for the Target Chamber (Fig. 14), the largest vacuum vessel to be set in the LTAB. The chamber was characterized by precision survey of the 48 indirect drive and direct drive beam/quad ports. A best fit of those port locations to the Target Chamber design model was used to value PSFs affixed to the chamber. Those PSFs in turn were used to perform final placement of the Target Chamber following installation into the building.

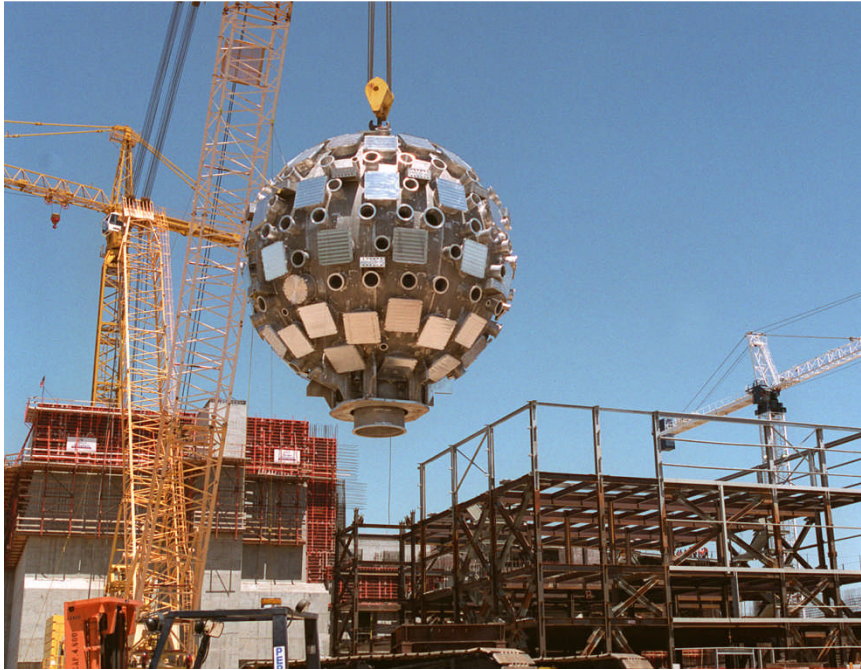


Fig. 14. The NIF target chamber was installed (2001) as part of building construction, with the roof installed afterwards. The covered square ports admit 4 beams each, 24 ports surrounding each pole. The equatorial square ports are for an alternative “direct target drive” configuration which may be used later in NIF’s life. The round ports are for diagnostics and alignment purposes, and the large port on the bottom is for maintenance access.

Component placement through direct survey of the LRU kinematic mounts was performed for the transport mirrors (LM4 – LM8) and the Periscope LRUs (PEPC, LM3/Polarizer, and LM2). The LM1 and LM3 Lightsource Launcher mounting plates (Lightsources described later), Preamplifier Transport System (PABTS) optical breadboards, optical mounts, Preamplifier kinematic mount rails, and numerous other components were directly positioned by precision survey. For each of these cases, a precision survey feature accurately referenced to the optical component, such as a pilot hole, an edge, or the mounting surface of a kinematic mount was directly adjusted to

OCD-derived coordinates. For the PABTS, we aligned a constellation of stops attached to the optical breadboards, against which the optical mounts were oriented during installation.

Commissioning Alignment

With the vessels, enclosures and kinematic mounts installed and aligned, the beamline was ready to receive the Line Replaceable units, or LRUs, and begin alignment. The types of optics LRUs [22] were mirrors, lenses, amplifier slabs, Plasma Electrode Pockels Cells (PEPC), spatial filter assemblies, and final optics. The LRUs operate in a clean/dry atmosphere to the TSF, and a 0.5”WG argon environment from SF4 to the Target chamber. The spatial filter structures operate in high vacuum ($<10^{-4}$ Torr), with the spatial filter lenses being the vacuum barrier. The spatial filter assemblies (‘Towers’) perform alignment, diagnostic, and wavefront functions at beam focus as well as spatial filtering during high-energy operation.

We followed a rigorous process of Installation Qualification (IQ) and Operational Qualification (OQ), guided by a Commissioning Flowchart construct for sequencing, tracking, and documentation. The flowchart sequence ensured prerequisites were met with an interactive and visual presentation. The IQ is a configuration-controlled procedure, used for initial functional testing of an installed LRU. The OQ is likewise configuration controlled, addressing a larger, more integrated aspect of operational activation usually involving two or more LRUs.

Initial beam alignment in the NIF was an extremely challenging project, particularly in the main (full aperture) section, as the beam is not accessible for alignment purposes. Basically, the beam is injected into the TSF pass 1 pinhole, is expected to perform 4 passes in the cavity, and reappear within $\pm 400 \mu\text{R}$ in the TSF pass-4 pinhole after 2 polarizer passes, 6 spatial filter pinhole passes, 8 mirror reflections, 10 spatial filter lens passes, 12 PEPC window/crystal passes and 54 amplifier slab passes, with a total propagation distance of 280m. The only permanent sensor for this alignment is a near/far-field camera in the Output Sensor Package (OSP), sampling the beam through an alignment beampath from an insertable 50% pickoff cube positioned behind either the TSF pass 1 or 4 pinhole. Because this sensor could not perform its function until light reached it, temporary alignment fixturing was designed and installed to facilitate commissioning alignment as minimum configurations of LRU's became available. The strategy for commissioning alignment systems is subdivided into the pre-amplifier, main-laser, relay optics, and transport to TCC (Fig. 15) and was executed as follows;

1. Beamline LRU installation.

To minimize the time required to 'find' beams within the beamline, mirrors were prealigned to their nominal angle offline, in the Optics Assembly Building [23] using a coordinate measuring machine, and installed as described in the references [22, 23].

Lens and mirror LRUs were installed to complete the beampath from LM1 to the TSF, including installation of the final spatial filter lens (SF4) immediately prior to the Switchyard. Temporary "Alignment Reference" spatial filter assemblies ('Reference Towers') were installed in the Cavity and Transport Spatial Filter locations, a total of 3

Towers per bundle of 8 beamlines (Fig. 16). We built only 2 each of these three types of Reference Towers, cycling them through each bundle during the initial alignment phase. These Reference Towers were utilized for five specific alignment commissioning operations described below. Due to the large quantity of laser slab LRUs undergoing installation, we started alignment without a full complement, however we did require an odd number of slabs installed to have the nominal beam centering offset from the Brewster's-angle mounted slabs.

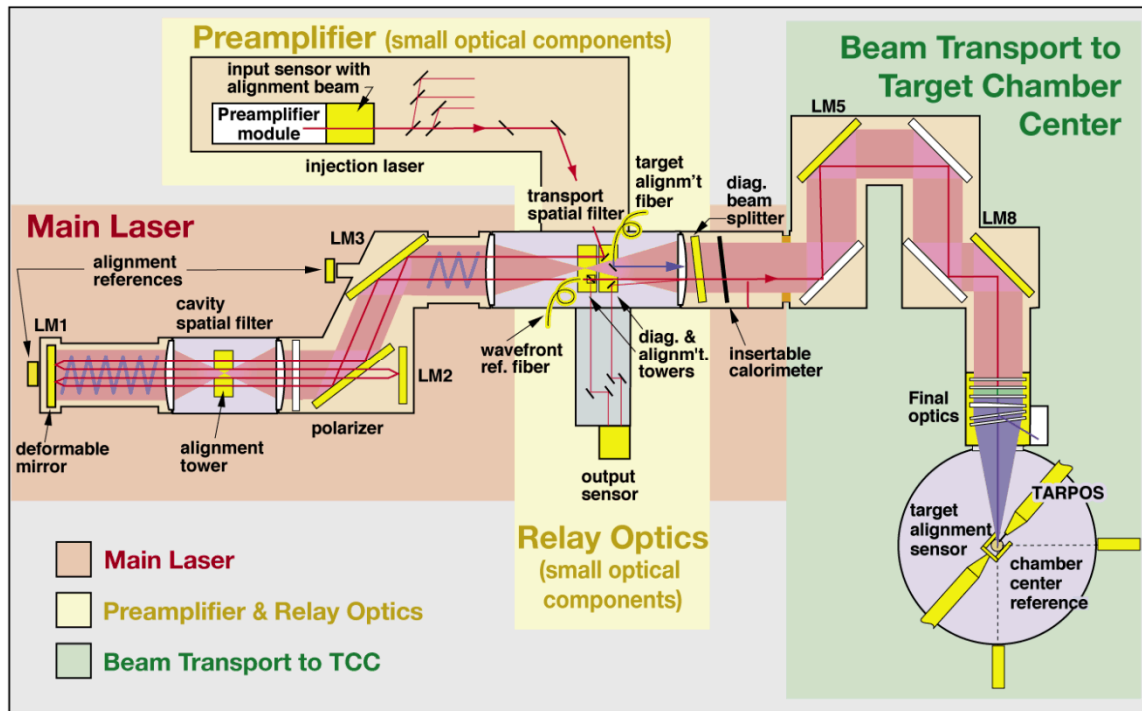


Fig. 15. Alignment commissioning was subdivided into the four regions of the Relay Optics, Preamplifier, Main Laser, and Beam Transport to TCC.

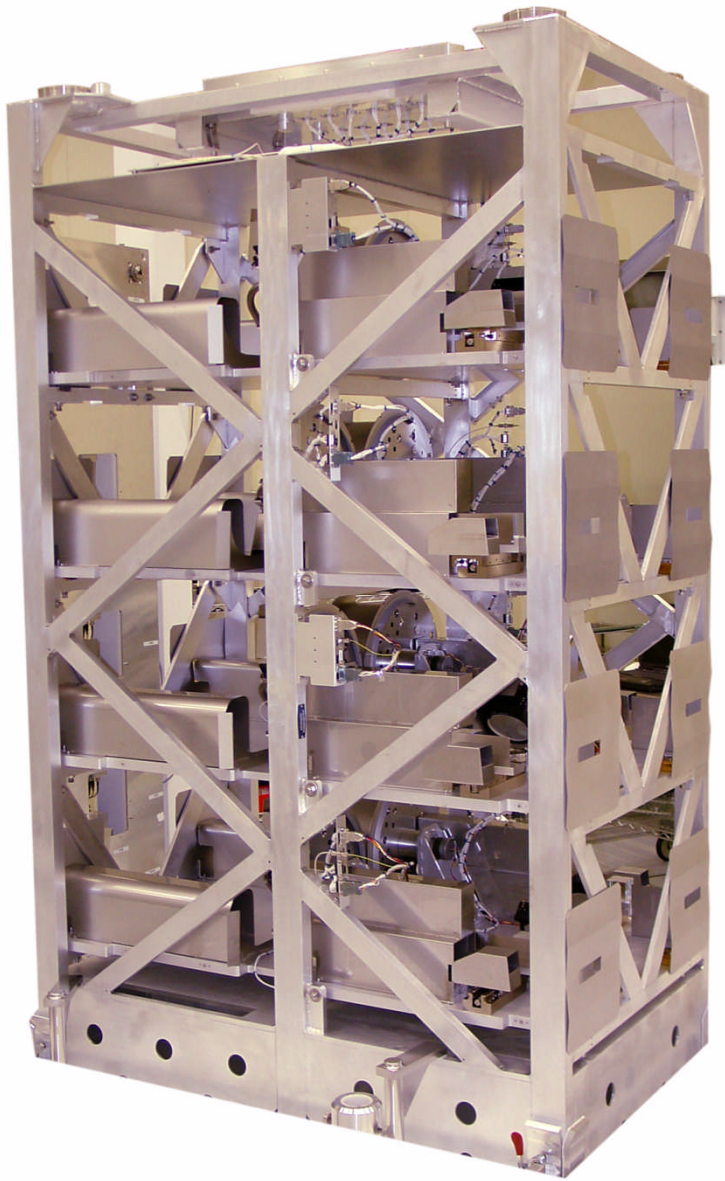


Fig. 16. A commissioning version of this Transport Spatial Filter Alignment Tower (TSFA) and the other two Tower types were used to commission main laser and relay optics alignment. Once the beamlines were commissioned, the shot-capable operations Towers were installed. The multitude of internal adjustments and calibrations required on each Tower LRU were performed off-line in a test stand surveyed and certified to replicate the on-line specifications.

2. Beamline pre-alignment

The Reference Towers were equipped with cameras, fiber sources, and illuminated references for beamline pre-alignment. The first prealignment step was to manually point the LM1 Lightsource and LM3 Lightsource centering references through the appropriate pinhole positions within the CSF (passes 2 & 4) and TSF (passes 1 and 4) respectively, using the Reference Tower cameras to detect the light. The Lightsources (described in Automatic Alignment, section 2) have a $\sim\pm 200\mu\text{R}$ divergence, but that was sufficient for LM3, LM2, and LM1 prealignment. This assured that light leaving the TSF pass-1 pinhole would return to TSF pass 4 with sufficient accuracy to be detected in the OSP and precision aligned after the operational TSF Towers were installed. Pass 2 & 3 are made possible during alignment by insertable half-wave plates near the CSF focus pinhole plane, rotating the beam polarization to transit the large-aperture polarizer. The same waveplates are in operational Towers for alignment operations. The TSFD Reference Tower source and camera were used to align the diagnostic beamsplitter reflected beam to its nominal location 2mR above TSF pass 4.

3. Relay Optics alignment

The Output Sensor acquires laser light through two independent channels (Fig. 15). One channel is called the “Alignment Path”, where 50% of the main beam is picked-off by an insertable splitter cube in the Alignment Tower (TSFA). Clearly this is practical only for low-power/low-energy beams as even the focused rodshot (PAM-only shot) beam would damage the splitter cube and Alignment Path relay optics. The “Diagnostics Path” is the other channel, using a 0.1% sample from the Diagnostics Beamsplitter (DBS) which is

mounted on the output side of the Transport Spatial Filter lens (SF4). The DBS reflection, which is 60mm above the outgoing beam at the TSF pinhole plane, is attenuated and routed down the Diagnostic Path relay optics. Both pathways were aligned during commissioning using the Reference Towers.

The Relay Optics is a very complex design, satisfying beam sampling and imaging requirements for alignment, wavefront, beam energy, beam power, and near-field profile. The alignment path for each beam has 9 optical elements per beamline, and the diagnostic path has 19 to image the beam sample to the OSP. On installation, the components were precision located, but additional lateral alignment in-situ was required for passive alignment into the OSP. The Reference Towers, designed to align these optical paths, originally utilized 1053nm laser sources from fiber launchers to project a pilot beam defining the nominal alignment and diagnostic beam path. Experience from aligning the first bundle demonstrated a fundamental weakness in this approach, as the required launcher pointing stability was not realizable. An alternative approach was developed and used for Relay Optics alignment, which involved precision surveyed targets at the OSP kinematic mount locations, survey instrumentation known as “Plummets”, and illuminated precision-survey positioned targets in the Reference Towers. The “Plummet” is designed to alternatively sight downwards to establish a vertical line-of sight to the surveyed OSP target, then upwards to continue along the same line-of-sight, to establish the two vertical and one horizontal leg for each of the Alignment and Diagnostic Relay Optic paths (Fig 17). The vertical path to the Tower was defined between surveyed, fiducialized blanks and the Reference Tower illuminated

fiducial. Finally, each of the optic mounts were laterally positioned using laser-scribed targets in each optic mount, one at a time, to the line-of-sight established between the “Plummet” and the illuminated Tower targets. The process was facilitated by modifying the “Plummet” with a CCD camera, both relieving the Alignment Technicians of sighting through an eyepiece and providing a means for documentation. The position for every optical mount was set and documented in this way, after which we populated the mounts with their respective optical components (lenses, mirrors, beamsplitters and attenuators). These optical components were manufactured and assembled with tight tolerances for mechanical to optical centers. The method was also used, with slight modification, to align the energy diode splitters into each beam’s integrating sphere/diode entrance aperture. No further alignment or magnification adjustments were required prior to operations except for the Wavefront Sensor optics.

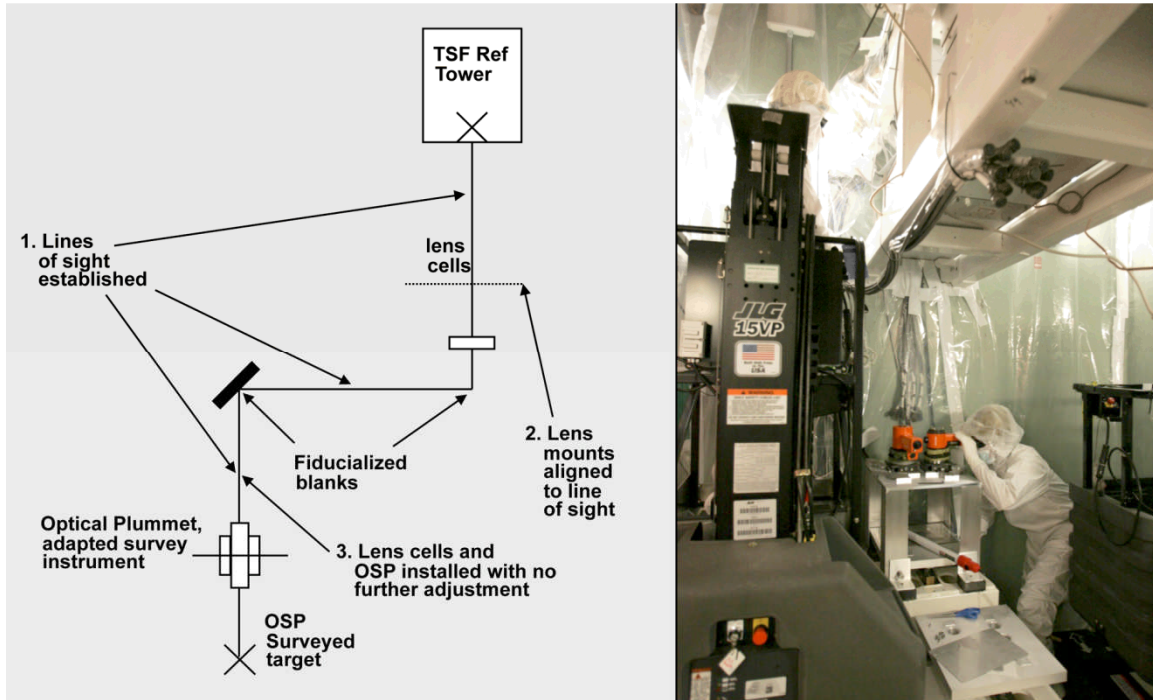


Fig. 17. Relay optics were positioned to lines-of-sight (LOS) established from the Output Sensor to the alignment and diagnostic Towers in the TSF. A modified survey instrument (“Plummet”) established the lower vertical LOS, and surveyed fiducialized blanks viewed through the Plummet established the other two LOSs to the illuminated Tower references. Two paths (one for alignment and one for diagnostics/wavefront) were commissioned for each beamline - 384 total.

4. Beam injection alignment

The operational TSFD Tower-mounted injection telescope and mirrors into pass-1 were pre-aligned prior to installation, with no on-line alignment requirement. The lower-injection mirror M9 (Fig. 8), however, was designed to be positioned to the Reference Tower injection path line-of-sight during commissioning. As this positioning requirement was not as stringent as the Relay Optics, the original Tower design utilizing fiber launchers mounted in the Reference Tower was sufficient. With the beam turned on, an aluminum fiducialized target mounted in the lower injection mirror mount was manually

positioned to be centered on the beam using an infrared viewer. The fiducial target was removed, the mirror installed, and adjusted to aim to a local crosshair on the horizontal leg for rough alignment. Later, when the PABTS was ready, a precision-surveyed crosshair was installed at the output mirror location of PABTS, and the Lower Injection mirror was used to point the Reference Tower beam to the crosshair. Likewise, when the alignment beam was available from PABTS, it was pointed back to the Lower Injection mirror local crosshair. With this completed, the PABTS beam was aligned into the main laser sufficiently well to commission the automatic alignment system.

After completing the above beam injection alignment and all the previously mentioned Reference Tower-aided alignments, we removed these Towers and installed the Operational Towers.

5. Preamplifier Beam Transport System Alignment

The Preamplifier Beam Transport System (PABTS) is built from conventional optical breadboards and components, with a combination of standard and custom mounts and all custom optics (Fig. 8). The optical breadboards are mounted vertically and were positioned using precision survey, onto which the precision surveyed ‘stops’ were mounted as previously discussed. The breadboards were populated with optical mounts set to the ‘stops’, with flats and mirrors installed and aligned using conventional methods (crosshairs, ISP alignment laser, and a camera mounted at the PABTS/Injection interface). The crosshairs positioned at various locations were grossly out of focus to the viewing camera, but the symmetric diffraction patterns permitted sufficiently accurate

crosshair center identification to meet our requirements generally $\pm 1\text{mm}$. As with all NIF commissioning, we executed a series of IQs and OQs, with data and documentation for each component's alignment saved for every beam. With the optical beam path established, the powered components (relay telescopes) were installed and aligned using conventional methods.

6. Automatic Alignment commissioning – main laser

Prior to sending beams to TCC, we finalized the alignment commissioning for the main laser, from the ILS to the switchyard wall, so that laser operational testing to the full aperture calorimeters (Fig. 15) could commence. The alignment was accomplished in several stages, following completion of all but laser slab installation, with the constraint that an odd number of laser slabs always had to be installed for alignment commissioning. For initial automatic alignment, we propagated the ISP-cw beam to the OSP camera, and created OSP focus and exposure settings for each of the alignment feedback loops (referred to henceforth as alignment 'loops'). The centering reference for each beamline is the LM3 lightsource launcher [24], with all centering loop image planes set to the LM3 lightsource. Likewise, the TSF pass-4 fiber source is the pointing reference for all the pointing loops. This follows a similar process, previously completed, for each Preamplifier module, with centering and pointing references contained in the ISP.

Since NIF's beams are square, we had a tight requirement on beam rotation (8mR) into the main laser. This rotation, due to unintentional out-of-plane reflections in the PABTS,

was corrected by shimming the PABTS timing trombone (not shown in Fig. 8) until the beam rotation matched the LM3 lightsource launcher. This had to precede wavefront control commissioning, to ensure adequate illumination of the Hartmann wavefront sensor [6].

Exposure settings (setpoints) for pointing loops were initially set without wavefront correction, as we faced the precedence that wavefront control could not be performed without aligned beams, yet final alignment commissioning required wavefront correction. Thus, after the initial main laser alignment, we commissioned wavefront control to correct the wavefront error at the output of SF4 to generally better than 1 μm (peak-peak). Following that, we completed commissioning of automatic alignment, including final exposure setpoint creation and fine-tuning for alignment loop cross-coupling, which is covered in the Automatic Alignment section.

7. Switchyard and Target Area transport mirror alignment

NIF was designed to center the beam at the final optics using corner-cube retroreflectors remotely inserted to the mechanically-established final optics aperture center. With the corner-cubes inserted, the incident ISP-cw beam is sampled by the cubes and counter-propagates through all 4 main-laser passes to pass 1, where the TSFA splitter cube picks-off the light to the OSP. The near-field position of the retroreflections is compared to the LM3-Lightsource pass-1 centering reference. Adjustments are made with mirrors LM5 and LM8 to center the spots, equivalently centering the outgoing beam at the final optics.

During commissioning, each transport mirror was adjusted using a version of this technique. There are 4 mirrors leading to the final optics (5 mirrors for 1/3 of the NIF beams), but only two are remotely actuated (Fig. 9). The rest are manually adjusted once during commissioning. Alignment was accomplished by inserting a plate with precision mounted and referenced corner cubes into the ‘guillotine’ slot, otherwise used as a protective cover for the mirror and beampath during mirror removal/replacement. The upstream mirror was adjusted, centering the corner cube reflections to the main-laser LM3-Lightsource centering reference as described above for the FOS. This process was performed serially to adjust each mirror from LM4 to LM7.

8. Final Optics alignment commissioning

After centering, the first step for pointing [6] to TCC was finding the beams on the chamber center Target Alignment Sensor or TAS. This sensor utilizes a 5mm × 7mm CCD. Thus pointing had to be within 350 μ R to acquire the alignment beam, a 375-nm lightsource from the TSFD [25,26]. The commissioning alignment of LM4-LM8 was sufficient to find the beam for approximately ½ the beamlines. A spiral search was required for the rest. There was never a problem finding the final optics corner cube reflections, which would require >20mR of pointing error before images of the centering references would be lost. Similarly, reflections from the second harmonic generation (SHG) and third harmonic generation (THG) KDP crystals were found in the OSP through an automatic-assisted spiral search. The 1053nm source for the SHG and THG alignment is at the TSF Alignment Tower fiber reference [26].

With beams approximately aligned to their respective sensors, we commissioned automatic alignment to TCC, creating camera attenuator and exposure setpoints and established cross-coupling to permit independent adjustments for beam centering, pointing, and the frequency conversion crystals.

Automatic Alignment

NIF Automatic alignment systems permit autonomous alignment for all 192 beams to the OSP in less than 10 minutes, and alignment to target chamber center in 44 minutes. Preamplifier alignment for all 48 PAMs consumes less than 5 minutes, and is performed in parallel with other, longer duration, tasks during the shot cycle. Beam and alignment reference features are extracted from CCD camera images (except for encoder loops). Therefore, to robustly identify alignment features for the large variety and quality of both beams and optical references, a significant image processing effort was made and sustained [27-33]. A gallery of representative images processed by this software is shown in Figure 18. For each automatic alignment loop, the reference image is acquired and alignment features are identified once. The beam image to be aligned is then acquired and its position is compared to the reference. Compensating mirror tilt actuations are made, and the process is iterated until the error is less than a predetermined amount specific to each alignment loop. The alignments are performed concurrently to the extent that shared resources permit (cameras, light sources), and to the extent that a certain alignment sequence must be followed. For example, alignment pointing to TCC proceeds in parallel with main laser alignment. Computation resources are distributed to permit parallel alignment while image processing uses a shared computational cluster.

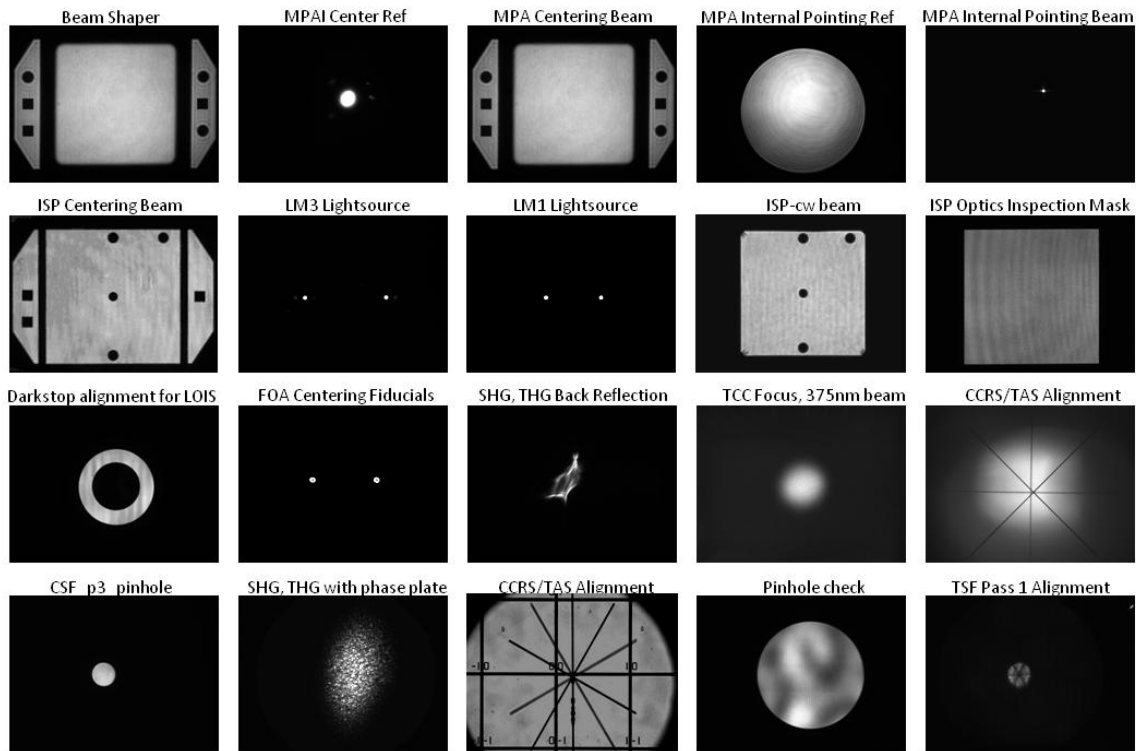


Figure 18. Gallery of images processed by the Automatic Alignment system during beam and target alignment. Images are acquired by CCD cameras in the ISP, OSP, Target Alignment Sensor, and Chamber Center Reference System.

There are three discrete partitions to NIF automatic alignment: preamplifier alignment, main laser alignment, and alignment to target chamber center. There is a centering and pointing handoff between each.

1. Preamplifier alignment

The preamplifier alignment for NIF is alignment of the PAM from the regenerative amplifier output relay plane (RP0, Fig. 7) to the ISP (Fig. 8). There is no active alignment within the regenerative amplifier, and the PAM cavity vacuum relay telescopes (VRTs)

are imaged to one another during commissioning with no further active alignment. The RP0 beam image is relayed through the PAM to the ISP relay plane, where pointing and centering are measured at the ISP.

Referring to Figure 7, there are 4 alignment locations, which are;

M4_{x,y} – centering at the MM4 M4_REF 980nm diode source, imaged at the ISP

VRT_{x,y} – pointing at the VRT-2 (and co-imaged VRT-1) pass-4 pinhole. The reference is the pinhole outline, illuminated by the 980nm diode source through MM4

RP8_centering_{x,y} – Beam centering measured at RP8, imaged to the ISP camera, the centering reference being a fixed obscuration mask in the ISP for the beam ‘wings’ (Fig. 18) extending outside the otherwise propagated square beam.

The associated actuators (mirror tip/tilt’s) to accomplish this positioning are linearly independent stepper motors on the mirrors and polarizers **BM1_{x,y}**, **MM1_{x,y}**, **POL1_{x,y}**,

RP8_pointing_{x,y} – Beam pointing measured at RP8, focused to the ISP camera, the pointing reference being a commissioning-established pixel address on the camera

and **POL3_{x,y}** (Fig. 7).

The response matrix for these measured locations and actuators is:

$$\begin{pmatrix} \mathbf{M4}_{x,y} \\ \mathbf{VRT}_{x,y} \\ \mathbf{RP8centering}_{x,y} \\ \mathbf{RP8pointing}_{x,y} \end{pmatrix} = \begin{pmatrix} \alpha & 0 \\ \alpha & \beta \end{pmatrix} \begin{pmatrix} \mathbf{BM1}_{x,y} \\ \mathbf{MM1}_{x,y} \\ \mathbf{POL1}_{x,y} \\ \mathbf{POL3}_{x,y} \end{pmatrix}$$

where each of the column vector elements are 2×1 vectors, and **α, β** are 4×4 response matrices.

While all 8 error parameters between beam and reference could be measured, followed by one adjustment of the 8 actuators determined by the inverse of the response matrix, in practice the α and β response matrices were separately measured during commissioning, and the inverse of each was used to close the control loops for the M4 centering, VRT pointing, RP8 centering, and RP8 pointing in sequence. This is the optimum approach because the time spent reconfiguring camera focus and exposure significantly exceeds mirror adjustment time as iterations are done. It takes less time to sequentially close the loops than to reconfigure the ISP for simultaneously iterating all 8 error terms. The pointing spot is a near diffraction-limited spot on the ISP camera, while the image for RP8 centering is shown in Figure 18, with the beam position and fixed centering reference contained in the ‘wing’ circular and square obscurations respectively. To improve accuracy and decrease loop closure time, the NIF control system is configured to remove mechanical backlash by always driving stepper motors in the same direction at the end of a move. This approach is used for all NIF alignment stepper motor actuators.

2. Main Laser Alignment

The Main Laser is aligned in 6 alignment loops, to the LM3 Light Source Launcher centering reference, and to the TSF pass-4 pointing reference. Alignment is performed working backwards from the TSF, with alignment of the ISP-cw beam performed last. For each loop, the source and reference laser light is transported to the OSP by the TSFA-mounted and actuated 50% splitter cube and associated relay optics [26]. First the reference image is acquired and processed to extract the reference position, then an image of the source undergoing alignment is acquired and processed to determine the error.

Iteration of motor moves and error measurement continue until the requisite error is reduced to its requirement.

Referring to the mirrors and sources shown in Figures 5,8,&19, a control matrix, was developed from the response matrix.

$$\begin{pmatrix} \text{LM1cent}_{x,y} \\ \text{CSFp4}_{x,y} \\ \text{CSFp3}_{x,y} \\ \text{TSFp1}_{x,y} \\ \text{ISPcwCent}_{x,y} \\ \text{ISPcwPoint}_{x,y} \end{pmatrix} = \begin{pmatrix} \alpha & 0 & 0 \\ \eta_1 & \beta & 0 \\ \eta_2 & \eta_3 & \gamma \end{pmatrix} \begin{pmatrix} \text{LM3}_{x,y} \\ \text{POL}_{x,y} \\ \text{LM1}_{x,y} \\ \text{LM2}_{x,y} \\ \text{M7}_{x,y} \\ \text{M9}_{x,y} \end{pmatrix}$$

As before, the column submatrices are 2×1 , and the response matrix submatrices are 4×4 . Unlike the PAM loops, the alignment sources change for each main laser alignment loop, while the centering and pointing references are unchanged. The inverse of each 4×4 response matrix permitted independent ‘cross-coupled’ actuations of each alignment pair. In addition, since centering requires much larger actuator moves, the inverse of the response sub-matrix cross-coupling moves were sufficiently accurate that pointing is performed after centering without inadvertent decentering outside the alignment requirements. The main laser response sub-matrix elements for η_1 , η_2 , and η_3 could be extracted from α and β , however this is irrelevant given that the sequence of alignments is equivalent to matrix solution by Gaussian elimination and they are not needed. We present first a description of the alignment references (Fig. 19) then discuss each alignment loop.

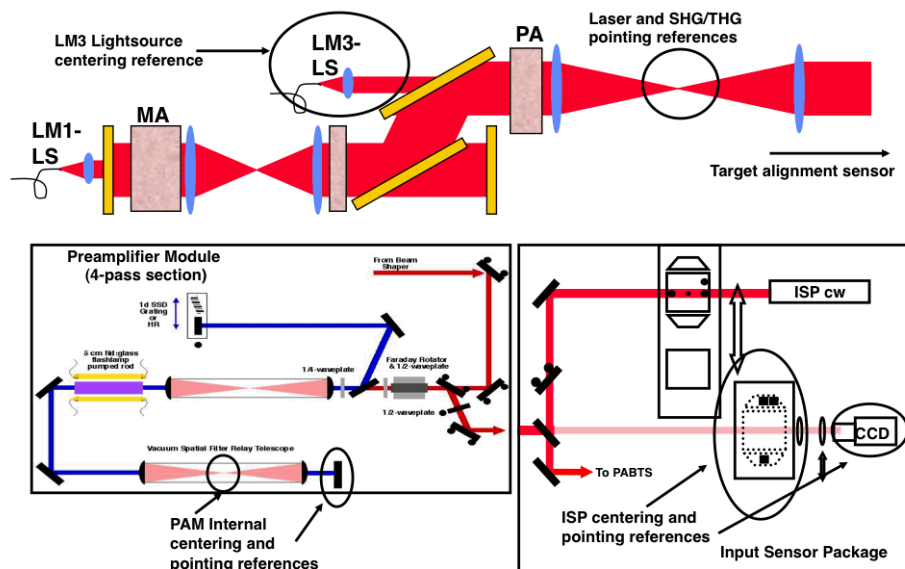


Fig. 19. Pointing and centering references for the NIF laser. Centering references are the PAM M4, ISP fixed reference, and the LM3 Lightsource. Pointing references are the PAM VRT-2 pinhole, ISP camera, TSF pass-4 pinhole, and the Target Alignment Sensor (not shown).

Centering reference: The main laser centering reference is the LM3 Lightsource (image shown in Fig 18), which launches 2 identical 1053-nm pairs of 13mm-diameter beams through LM3 (partial transmission of vertically polarized light), through the TSF and into the OSP. The two beam pairs are pointed so as to propagate to TSF pass-4 and TSF pass 1 respectively, with the pass-4 beam pair being the main laser centering reference. The pass-1 pair is the final optics centering reference as well as the TSF pass-1 source for one of the Main Laser alignment loops (below). The centering reference is designed so that the pass-1 and pass-4 beams overlap at the pass-1/pass-4 crossover relay plane shown in Figure 12.

Pointing reference: A diffraction limited 1053nm source mounted to the TSF pinhole wheel [26] is the main laser pointing reference. The pinhole wheel, besides carrying a selection of 100- μ R, 150- μ R and 200- μ R pinholes, has several positions dedicated to alignment, wavefront, and optics inspection functions that are rotated into position as required. The pointing reference uses light from the same beam's ISP coupled into a fiber. The fiber is routed to the TSF and the light is launched at the TSF pass 4 focus. It also serves as the reference source for wavefront control. In the same pinhole wheel position, a second fiber-based source, also fed from the ISP, is positioned to provide a pointing reference for frequency converting crystal alignment (below).

The six separate alignment loops for main laser alignment are:

LM1 Centering, CSF pass-4 pointing (α response matrix): The LM1 Lightsource, (image in Fig. 18) launches a pair of 13mm beams spaced by 171mm switched exclusively to either the CSF pass 4 or CSF pass 2 pinholes. The center point between the pass-4 beam pair is aligned by tilting the LM3 and Polarizer to match the center point of the LM3 Lightsource. For pointing, the circular outline of a small (50 μ R) pinhole rotated into the CSF pass 4 position and back-illuminated by the LM1 Lightsource is aligned to the above-described TSF pass-4 pointing reference using the LM3/Polarizer gimbal pair.

CSF pass 3 pointing, TSF pass 1 pointing (β): This loop pair uses LM1 to align first the CSF pass-3 back-illuminated pinhole outline, using LM1 lightsource illumination reflected off LM2, to the TSF pass 4 reference. Then, the TSF pass 1 pinhole illuminated

by the LM3 Lightsource and retroreflected in the forward direction through the CSF to TSF pass-4 is adjusted by LM2 to match the TSF pass-4 pointing reference.

With the completion of this second alignment loop pair, the main laser alignment is complete, with no further free parameters. The alignment to CSF passes 1 and 2 are entirely determined by the alignments to TSF pass-4, CSF pass-4, CSF pass-3, and TSF pass-1. Installation placement or lens manufacturing errors impose pointing errors on the otherwise uncontrolled CSF passes 2 and 1, however the design tolerance keep these misalignments to well within specifications. We control alignment to TSF pass 4 and CSF pass-4 because they are the highest fluence passes, and we control to TSF pass-1 because it is the smallest pinhole (100 μR vs. 200 μR for the rest). The choice of aligning CSF pass-3 vs. using CSF pass 2 as the only remaining controlled pass was convenience, since the alignment of the pass-3 pinhole image is independent of LM2 actuation.

ISP-cw beam injection centering and pointing (γ response matrix): Prior to injection through the Preamplifier Beam Transport, the ISP-cw 1053nm beam is aligned to the same ISP centering and pointing references as the Preamplifier module (Fig. 8). The ISP-cw beam is subsequently used for this main laser loop pair and 3 other alignment loops to the final optics. For this loop pair, the ISP-cw beam is transported from the ISP references to the M7 mirror via commission-aligned preamplifier beam transport optics. Mirrors M7 and M9 align the ISP-cw beam centering to the LM3 Lightsource reference, and point to the TSF pass-4 reference using a control matrix derived from an inverse of

the γ response matrix. With the completion of this final alignment loop, the NIF beamlines are aligned from the PAM through to the TSF switchyard mirror LM4.

3. Alignment to Target Chamber Center

Each laser beam exiting the laser bay is remapped from the rectangular beam arrangement to the required spherical geometry in the NIF switchyard (Fig 9). A sequence of either 4 or 5 mirrors transports each beam to a position at the target chamber. Actuated mirrors LM5 and LM8 comprise the centering and pointing gimbal to first center the beam to insertable fiducials located at the FOS vacuum window, then point the beam to the specified aim point at target chamber center. Focus is adjusted a-priori based upon a calculation of the aim point. The aim point varies based upon target requirements up to 4mR (3cm) away from target chamber center, which far exceeds the allowed 10 μ R alignment tolerance for the second- and third-harmonic-generating crystals (SHG, THG). As a consequence, the SHG and THG are cross-coupled so as to maintain the proper angle relative to the input beam when it is aimed away from TCC. The cross-coupling is derived from the response matrix:

$$\begin{pmatrix} \text{FOAcent}_{x,y} \\ \text{TCCpoint}_{x,y} \\ \text{SHGpoint}_{x,y} \\ \text{THGpoint}_{x,y} \end{pmatrix} = \begin{pmatrix} \alpha & 0 \\ \gamma & \beta \end{pmatrix} \begin{pmatrix} \text{LM5}_{x,y} \\ \text{LM8}_{x,y} \\ \text{SHG}_{x,y} \\ \text{THG}_{x,y} \end{pmatrix} \beta = \begin{pmatrix} \beta_1 & \beta_2 & 0 & 0 \\ \beta_3 & \beta_4 & 0 & 0 \\ 0 & 0 & \beta_5 & \beta_6 \\ 0 & 0 & \beta_7 & \beta_8 \end{pmatrix}$$

where

Alignment to TCC is accomplished in the order of the response matrix, implemented as follows:

Beam centering to the Final Optics System (FOS) (α): Physical center of the FOS is mechanically defined as midpoint between two precision corner-cube retroreflectors mounted to a fiducial arm that inserts at the FOS vacuum window on the air side. The ISP-cw light propagated from the injection laser system is incident upon the retroreflectors, creating two ‘beamlets’ counterpropagating back through the main laser to TSF pass-1 where it is sampled. Picked-off by the TSFA pass-1 positioned splitter cube, it is imaged at the OSP near-field camera. The reference for this centering is the LM3 Lightsource, pass-1, described earlier. Using the control matrix, an inverse of the response submatrix α , LM5 and LM8 are adjusted to meet centering requirements.

Beam pointing to TCC (α): Beams may be pointed as far as 30mm from TCC. For a target shot, the responsible scientist specifies the desired aim points in a target chamber Cartesian coordinate system with its origin at TCC. The z axis is vertical and corresponds to the z axis of the Target Alignment Sensor (TAS) [6] when the TAS is in its nominal TCC position, with y pointing back towards the main laser system.

For a given TAS alignment location away from TCC, the calculated intersection of a beam on the TAS camera when the beam is aligned to its desired aim point is the TAS alignment goal for that beam. TAS, which is calibrated in the same coordinate system, detects the beam, and the control system adjusts LM5 and LM8 based upon the same α^{-1}

control matrix as the centering above. If the pointing projection is off the TAS camera, TAS is repositioned for the beam or group of beams offset in the (x,y) plane from TCC.

The final lenses are designed to focus 351-nm light to chamber center. The 1053-nm ISP-cw light could not be used for alignment because it focuses 46cm past TCC and is 16mm laterally offset by design. An intermediate (375nm) wavelength source [25] is utilized for pointing to TCC. This is accomplished using a kinematic insertable mirror near the focus of the Transport Spatial Filter system [26], which launches the alignment beam to TCC with a longitudinal and slight lateral offset so it focuses at TCC. Motor stages in the Transport Spatial Filter permit fine adjustment of the launched position, permitting precision co-alignment between the 375nm beam and the 351nm beam at TCC. Transport mirrors LM4 – LM8 are designed to minimize reflection of 351nm light due to backscatter concerns; so using a 351nm alignment source was not feasible. Through a series of rod-shots fired to TAS (main amplifier not pumped), the 375nm lightsource launcher position is adjusted to match the 351nm focused spot from the pulsed beam at TAS.

Second harmonic and third harmonic crystal tuning/alignment: The SHG and THG crystals are cut for nominal 10530.1Å tuning when the SHG second surface face normal is 580 μR from the incident beam, and the THG face normal is oriented 10.58mR from the incident beam. The alignment of each crystal is performed by first observing the reflection from its coated surface and pointing to the reference fiber in the TSFA. Then the crystal is offset to the required alignment using optics-mount position encoders which report SHG or THG relative crystal angle in two axes. Angle offsets due to manufacturing tolerances, temperature, operational wavelength changes, and other

sources are combined into one offset adjustment for each of the SHG and THG. Each is controlled by the inverse of the 2×2 response submatrices $(\beta_1-\beta_4)$.and $(\beta_5-\beta_8)$ respectively. Since this is the final beam alignment function, there is no need to further adjust the crystals due to upstream pointing modifications.

5. Alignment Performance

The critical performance measures for alignment include time to align and pointing accuracy. Alignment time affects shot cycle time; pointing and centering accuracy within the main laser must be sufficient for machine-safe and repeatable laser operation; and alignment to TCC is critical for target performance. Statistics on 192-beam shots show that PAM alignment time averages 4.2 min, Main Laser 9.7 min, and alignment to TCC 44 minutes, which is acceptable. However, improvements such as interleaving image acquisition are ongoing with a goal of 25 minutes for TCC alignment.

Pointing performance to the target is measured on a dedicated shot. A silicon target is used for this purpose; 8.3mm square, 50 μ m thick, and overcoated with 1 μ m of gold. A 7×8 array of pointing locations is defined on the target, and individual top beams assigned to 52 of these locations, where four of the locations have 40 μ m holes for top/bottom registration, orientation, and scale. The laser is set up for low-energy, short-pulse operation (35J, 100ps). X-ray emission from the illuminated spots is recorded by a top-viewing static x-ray imaging camera [34]. A similar arrangement is implemented for beams on the bottom side of the target. The four unassigned locations on top have 40mm holes and are illuminated by the bottom beams for registration, orientation, and scale.

The upper SXI camera image for a shot on 6/22/10 is shown in Fig. 20, and analysis shows a pointing error of 56 μm RMS to the beams' aim points in the plane of the target, which translates to less than 50 μm normal to each beam, meeting the requirement [12].

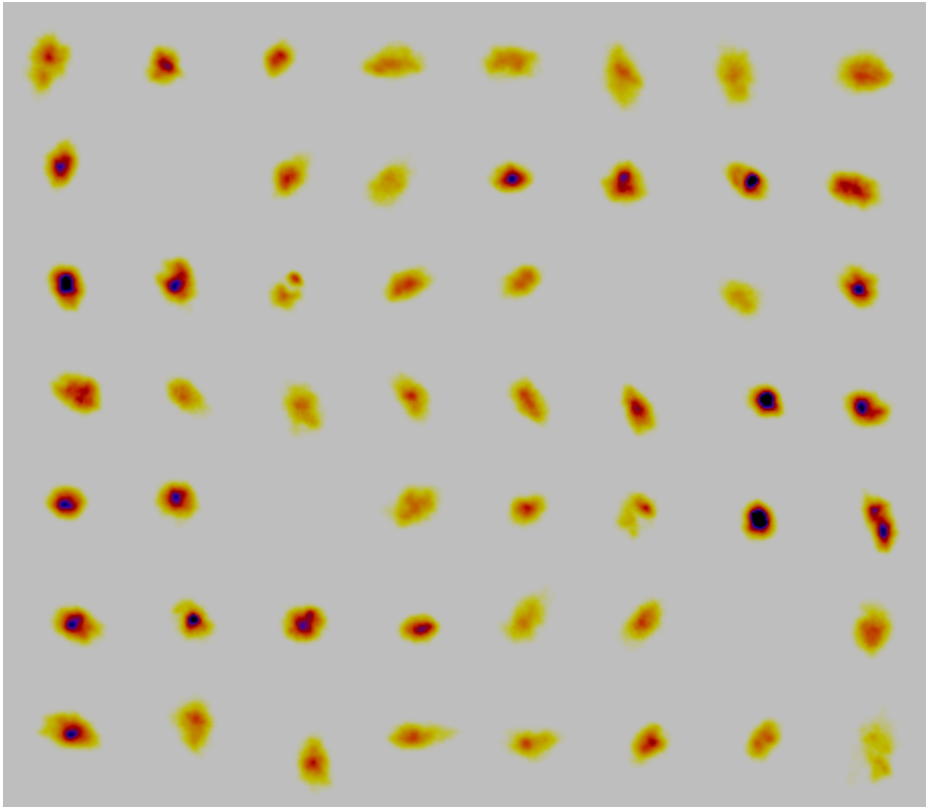


Figure 20. Static X-ray imaging (SXI) camera image for the NIF pointing validation shot. 48 upper and 48 lower beams are pointed to coordinates on a flat Au-coated Si target. An additional 4 bottom (not shown) and 4 top beams on target holes provide registration and scale. A shot is fired with a 100-ps pulse and the X-ray image captured as shown for the upper SXI. An equivalent image is taken for the lower SXI.

Now completed, the NIF is proceeding on its mission as the Inertial Confinement Fusion Facility, and experiments are proceeding. A summary of results obtained between August and December, 2009 is presented in reference [35].

6. Acknowledgements

The authors would like to thank the countless professionals including LLNL employees, supporting contractor individuals, and vendors who participated in the NIF project for their effort and dedication. Projects such as NIF require engineering support in all disciplines, physics expertise, conventional facility specialists, electrical and mechanical crafts, and administrative support in all areas of management, financial, procurement. The support and great effort by all have combined to make NIF the success it is, and bring it to the point where Inertial Confinement Fusion experiments leading to target ignition can commence.

This work performed under the auspices of the U.S. Department of Energy by Lawrence Livermore National Laboratory under Contract DE-AC52-07NA27344.

7. References

1. Miller, G. H., Moses, E. I., & Wuest, C. R., "The National Ignition Facility," *Optical Engineering: the Journal of the Society of Photo-Optical Instrumentation Engineers* **43** (12), 2841 (2004).
2. Spaeth, M. L., Manes, K. R., Widmayer, C. C., Williams, W. H., Whitman, P. K., Henesian, M. A., et al., "National Ignition Facility wavefront requirements and optical architecture," *Optical Engineering: the Journal of the Society of Photo-Optical Instrumentation Engineers*. **43** (12), 2854 (2004).
3. Tietbohl, G. L., & Sommer, S. C., "Stability design considerations for mirror support systems in ICF lasers," *Proceedings- SPIE The International Society for Optical Engineering*. [3047-94], 649-660 (1997).
4. J. D. Lindl, P. Amendt, R. L. Berger, S. G. Glendenning, S. H. Glenzer, S. W. Haan, R. L. Kaufmann, O. T. Landen, and L. J. Suter, "The physics basis for ignition using indirect-drive targets on the National Ignition Facility, " *Phys. Plasmas* **11**, 339-491 (2004).
5. Bowers, M., Burkhart, S., Cohen, S., Erbert, G., Heebner, J., Hermann, M., et al., "The injection laser system on the National Ignition Facility," [6451-55]. *Proceedings- SPIE The International Society for Optical Engineering*, 6451-55, (2007).
6. R. A. Zacharias, N. R. Beer, E. S. Bliss, S. C. Burkhart, S. J. Cohen, S. B. Sutton, R. L. Van Atta, S. E. Winters, J. T. Salmon, M. R. Latta, C. J. Stolz, D. C. Pigg, and T. J. Arnold, "Alignment and wavefront control systems of the National Ignition Facility," *Opt. Eng.* **43**, 2873-2884 (2004).

7. Rhodes, M. A., Fochs, S. N., Bilotft, P. J., Alger, T. W., Funkhouser, B., & Boley, C. D., "Plasma electrode Pockels cell for the National Ignition Facility," *Proceedings- SPIE The International Society for Optical Engineering*. [3492-56], 144-147 (1999).
8. Dixit, S. N., Feit, M. D., Perry, M. D., & Powell, H. T., "Designing fully continuous phase screens for tailoring focal-plane irradiance profiles," *Optics Letters* **21** (21), 1715, (1996).
9. Auerbach, J. M., Wegner, P. J., Couture, S. A., Eimerl, D., Hibbard, R. L., Milam, D., et al., "Modeling of frequency doubling and tripling with measured crystal spatial refractive-index nonuniformities," *Applied Optics* **40**, 1404-1411 (2001).
10. Haynam CA, Wegner PJ, Auerbach JM, Bowers MW, Dixit SN, Erbert GV, et al., "National Ignition Facility laser performance status," *Applied Optics* **46** (16), 3276-303 (2007).
11. (***NIF Requirement 5500902-OC***) "Laser system beam control & diagnostics shall point the main laser beam to center of CSF pass1 and CSF pass2 shot pinhole locations with an accuracy of better than 10% of the pinhole diameter. Laser system beam control & diagnostics shall point the main laser beam to center of CSF pass3, CSF pass4, TSF pass1 and TSF pass4 shot pinhole locations with an accuracy of better than 5% of the pinhole diameter."
12. (***NIF Requirement 5500905-OB***) "For each shot, position each beam at any location within 5cm of target chamber center such that the rms deviation of all beams from their specified positions is 50 μ m or less when measured perpendicular to the beam propagation directions. No single beam shall deviate more than 200 μ m. This

requirement applies equally to all beams whether directed at the principal target or at equatorial backlighting targets. The accuracy of surrogate alignment shall be periodically validated by direct detection of low level pulses.”

13. Sommer, S. C., & Bliss, E. S., “Beam positioning,” *Proceedings- SPIE The International Society for Optical Engineering*. (3492), 112-135 (1999).
14. Noble, C.R., & Hoehler, M.S., S.C. Sommer, “*NIF Ambient Vibration Measurements*,” <http://www.osti.gov/servlets/purl/802614-CVlu1A/native/> (2002).
15. Kemple, P., “*Vibration Measurements at NIF Site*,” NIF Project Internal Report, *NIF-0062282*, Feb 6, 2001.
16. Tabatabale, M., Sommer, S., “Analysis of Soil-Structure Interaction Due to Ambient Vibration,” *ASME -PUBLICATIONS- PVP*, **364**, 397-406 (1998).
17. Tietbohl, G. S., Sommer, S.C., “*Stability design considerations for mirror support systems in ICF lasers*,” LLNL report UCRL-JC-125396, prepared for the 2’nd Annual International Conference on Solid-State Lasers for Application to Inertial Confinement Fusion, Oct 22, 1996, **osti** <http://www.osti.gov/bridge/purl.cover.jsp?purl=/471333-QXPIoZ/webviewable/>
18. English, R. E., Laumann, C. W., Miller, J. L., & Seppala, L. G., “Optical system design of the National Ignition Facility,” (Invited Paper) [3482-106], *Proceedings- SPIE The International Society for Optical Engineering*, (3482) 726-736 (1998).
19. English, R. E., “Clear aperture budget for main laser system (LM1 – SF4),” NIF-0000475, Aug 19, 1996 (internal NIF document)

20. Burkhart, S. C., “Component placement and optical tolerancing requirements,” NIF-0053005, Aug 16, 2000 (internal NIF document)
21. Burkhart, S. C., “NIF Clear Aperture – optical component placement tolerance revalidation,” NIF-5007159, Nov 14, 2000 (internal NIF document)
22. Larson, D. W. “NIF laser line-replaceable units (LRUs),” *Proceedings- SPIE The International Society for Optical Engineering*. [5341-12] 127-136 (2004).
23. R. E. Bonanno, “Assembling and installing line-replaceable units for the National Ignition Facility,” *Opt. Eng.* **43** 2866-2872 (2004).
24. Bliss, E. S., Feldman, M., Murray, J. E, Vann, C. S., (1995), Laser chain alignment with low-power local light sources, *Proceedings- SPIE The International Society for Optical Engineering*,. 2633, 760-767
25. English, R. E., Seppala, L. G., Vann, C. S., & Bliss, E. S., “Use of an intermediate wavelength laser for alignment to inertial confinement fusion targets,” *Proceedings- SPIE The International Society for Optical Engineering*. 2633, 604-607 (1995).
- AUTHOR’s NOTE: The NIF design was modified from the 389nm source listed in this paper to a 375-nm source.
26. Holdener, F. R., Ables, E., Bliss, E. S., Boege, S. J., Boyd, R. D., Chokol, C. J., et al., “Beam control and diagnostic functions in the NIF transport spatial filter,” [3047-100]. *Proceedings- SPIE The International Society for Optical Engineering* (3047), 692-699 (1997). AUTHOR’s NOTE: The “ 3ω sampled beam diagnostic” referenced herein was eliminated from the design for reasons of protection from 351-nm backscattered light. In addition, the TSF reticle functions were no longer required and were eliminated.

27. K. Wilhelmsen, A. Awwal, W. Ferguson, B Horowitz, V. Miller Kamm, C. Reynolds, "Automatic Alignment System For The National Ignition Facility," *Proceedings of 2007 International Conference on Accelerator and Large Experimental Control Systems (ICALEPCS07)*, 486-490, Knoxville, Tennessee, (2007). <http://accelconf.web.cern.ch/accelconf/ica07/PAPERS/ROAA02.PDF>
28. W. A. McClay III, A. A. S. Awwal, S. C. Burkhart, J. V. Candy, "Optimization and improvement of FOA corner cube algorithm," in *Photonic Devices and Algorithms for Computing VI*, edited by K. Iftekharuddin and A. A. S. Awwal,, Proc. of SPIE 5556 , pp. 227-232. (SPIE Bellingham, WA 2004)
29. A. S. Awwal, J. V. Candy, C. A. Haynam, C. C. Widmayer, E. S. Bliss, and S. C. Burkhart, "Accurate Position sensing of defocused beams using simulated beam templates," in *Photonic Devices and Algorithms for Computing VI*, edited by K. Iftekharuddin and A. A. S. Awwal, Proc. of SPIE 5556 , pp. 233-242 (SPIE Bellingham, WA 2004).
30. A. A. S. Awwal Kenneth L. Rice, Tarek M. Taha, "Fast implementation of matched-filter-based automatic alignment image processing," *Optics & Laser Technology*, **41** 193-197 (2009).
31. A. A. S. Awwal, Wilbert A. McClay, Walter S. Ferguson, James V. Candy, Thad Salmon, and Paul Wegner, "Detection and Tracking of the Back-Reflection of KDP Images in the presence or absence of a Phase mask," *Appl. Opt.* **45** 3038-3048 (2006).

32. A. A. S. Awwal, Kenneth L. Rice, Tarek M. Taha, "Hardware accelerated optical alignment of lasers using beam-specific matched-filters," *Applied Optics*, Vol. 48, pp. 5190-5196 (2009).
33. Candy, J. V., McClay, W. A., Awwal, A. A. S., & Ferguson, S. W., "Lasers and Laser Optics - Optimal position estimation for the automatic alignment of a high-energy laser," *Journal of the Optical Society of America. A, Optics, Image Science, and Vision* **22** (7), 1348 (2005).
34. Koch, J. A., Alvarez, S. S., Bell, P. M., Lee, F. D., Moody, J. D., & Landon, M. D., "Design of the National Ignition Facility static x-ray imager," *Review of Scientific Instruments*, **72**, 1, 698 . (January 01, 2001).
35. MacGowan, B. J., Michel, P., Meezan, N. B., Suter, L. J., Dixit, S. N., Kline, J. L., Kyrala, G. A., ... Glenzer, S. H., "Symmetric Inertial Confinement Fusion Implosions at Ultra-High Laser Energies," *Science*, 327, 5970, 1228 (March 05, 2010).